Theoretical Linear and Nonlinear Rheology of Symmetric Treelike Polymer Melts

Richard J. Blackwell,*,†,‡ Oliver G. Harlen,† and Tom C. B. McLeish‡

Department of Applied Mathematics, University of Leeds, LEEDS LS2 9JT, UK, and IRC in Polymer Science and Technology, University of Leeds, LEEDS LS2 9JT, UK

Received September 28, 2000

ABSTRACT: Molecular calculations for the rheological behavior of a melt of multiply branched polymers with three levels of branching are presented. Extending the Doi−Edwards−de Gennes tube model, we consider a relaxation hierarchy where the entangled chains relax from the outermost sections toward the center of a branched treelike molecule. Generalizing star−polymer dynamics gives relaxation times in linear response. By including stretching of segments, predictions are made for the stress in nonlinear response. Relative motion between tube and polymer chain is included in the orientation dynamics. The novel constitutive equation we propose predicts characteristic features in the nonlinear rheology. These features arise from coupling of the stretch and orientation in different sections of the molecule. Such coupling and relative tube-chain motion are not present in existing molecular theories yet may be significant in the rheology of multiply branched polymers such as low-density polyethylene. The full tube-model calculation is compared to a "multimode pom-pom" model of the same architecture, illuminating the approximations made in that approach.

1. Introduction

Powerfully predictive theories for the relaxation mechanisms of branched polymers in entangled melts have been developed recently on the basis of the Doi−Edwards−de Gennes tube model. Notably theories for stars[1] and H-polymers[2] give quantitatively accurate predictions for the linear and even nonlinear rheology. The theories are based around the concept of topological constraints forming an effective "tube".[3] An ultimate goal is to generalize the existing tube theories to polymers with arbitrary branching structures. Strong indications that this is possible are suggested by the success of an approach to the multiply branched LDPE that models the melt as a "decoupled" blend of "pom-pom" molecules.[4,5] The reasons for the effectiveness of this model are not entirely clear—a full treatment of multiply branched molecules is clearly warranted. Hierarchically, the next topology to consider is a three-level Cayley tree. This highly symmetrical branched structure contains three segment types. Whereas the pom-pom neatly separates into "arms" and a single "cross-bar", the Cayley tree has a hierarchy of arms upon arms (see Figure 1). The symmetry of the Cayley tree demands that all arms in each level are identical. This symmetry simplifies the calculation of the relaxation dynamics of the polymer; however, the qualitative behavior of asymmetric molecules should be similar.

In branched polymers, reptation of molecular segments is inhibited by the presence of branch points. Segments are forced to disentangle via fluctuation modes of the entangled path length.[3] Consequently, chain segments close to free ends relax first, freeing themselves from their tube constraints. Once the free end has relaxed back to the branch point, the next segment is free to move. The effect of the outer segments is to provide a large frictional resistance at the branch point. This hierarchical relaxation process continues toward the inner segments of the molecule. The outermost segments of both pom-pom and Cayley tree molecules behave like star arms in a fixed entanglement network. However, in the three-level Cayley tree, the pom-pom backbone is replaced by two further layers of starlike arms. Following the relaxation hierarchy, these arms relax on successively longer time scales. Pom-pom backbone relaxation is similar to a linear polymer, with reptation modified to account for the dominating branch point friction. Similarly, the inner segments of Cayley tree polymers relax as modified star arms.[6]

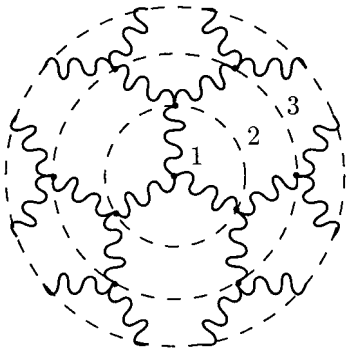

Figure 1. A three-level Cayley tree. The three different segment types are labeled from the center out to the free end. The example shown here has $n = 3$ and $q = (3, 2, 2)$.

The linear viscoelastic behavior of star polymers may be calculated[1] using a relaxation time defined as the first passage time of the free end along the tube contour. We generalize this approach to all segments in a Cayley tree by using the dominant friction at the branch point. This gives the linear viscoelastic moduli for the Cayley tree. The nonlinear viscoelasticity of star polymers follows the same strain dependence as linear polymers[7] due to the alignment effect of the flow on the polymer chains and the inability of flow to induce significant stretch in chains with a free end. However, in branching topologies with more than one branch point, such as the pom-pom and Cayley tree, molecular segments trapped

† Department of Applied Mathematics.
‡ IRC in Polymer Science and Technology.

10.1021/ma001687a CCC: $20.00
Published on Web 03/13/2001

between branch points can stretch. This removes time strain separability from the resulting constitutive equation.[8] Stretching also gives the extension hardening property of branched polymers.[9]

To calculate the contribution to the stress, it is necessary to know both the stretch and orientation distribution of molecular segments. The orientation distribution is a continuous function of the position along the contour of the molecule, and its evolution is controlled by the starlike relaxation. Conversely, the stretch of all molecular segments between two adjacent branch points is the same (since any variations are relaxed on the scale of local Rouse times), so that stretch is a piecewise constant function. In the pom-pom model, the orientation distribution in the cross-bar is also treated as being independent of position. However, such an approximation cannot be made for the Cayley tree, due to the exponential variation of the relaxation time with position.

In this paper we calculate relaxation times for the entangled Cayley tree polymer and derive a constitutive equation. Just as the simpler pom-pom architecture gave rise to a novel constitutive equation, so the Cayley tree architecture produces a constitutive equation of higher complexity. This constitutive equation is *not* just a simple generalization of the pom-pom equations. In the next section we introduce the notation for this paper and state the results from Doi−Edwards theory that are essential for this work. In the following section branch point dynamics are introduced. Using "dynamic dilution" (Appendix A), we derive the relaxation times in section 3. The constitutive equation is proposed in section 4. Finally, we give predictions of the model in both linear and nonlinear flows and make comparisons to the cruder multimode pom-pom approximation.

1.1. Tube Theory. De Gennes' tube concept highlights the importance of topology in polymer melts. This tube concept was used to great effect by Doi and Edwards[3] to calculate melt stresses in entangled linear polymers. We present full molecular calculations for the melt stress of entangled Cayley tree polymers using the Doi−Edwards framework. Necessary results from Doi and Edwards are summarized below, together with the notation we use for the Cayley tree.

Doi−Edwards'[3] theory for stress relaxation in entangled polymers is based on the concept of a primitive chain. The polymer melt is an ensemble of many polymer chains, the dynamics of which may be elicited by considering a single typical chain. Dynamics on length scales smaller than an entanglement spacing are neglected by replacing the chain with the corresponding "primitive chain". The primitive chain is the shortest path with the same topology through the entanglement network and the same end-to-end vector as the polymer chain. The intrinsic properties of the polymer are represented by the Rouse model parameters: number of Rouse beads, N, Kuhn step length, b, and bead friction coefficient, ζ_0. In tube theories we use the Rouse time of an entanglement segment, $\tau_e = \zeta_0 N_e^2 b^2/3\pi^2 kT$, as a fundamental time scale (where N_e is the number of Rouse beads in an entanglement segment). If z' is a distance along the primitive chain contour from the center of the molecule and $\mathbf{R}(z',t)$ the position of the primitive chain,

$$\mathbf{u}(z',t) = \frac{\partial}{\partial z'}\mathbf{R}(z',t) \tag{1}$$

is a unit vector tangent to the primitive chain. From the property of Gaussian chains the mean primitive chain contour length, $\bar{z}$, is given by

$$\bar{z}a = Nb^2 \tag{2}$$

where a is the step length of the primitive chain. The two step lengths are related by

$$a^2 = \frac{3}{\nu}N_e b^2 \tag{3}$$

The numerical factor ν is found to be 15/4 by taking the small strain limit of the Doi−Edwards $\mathbf{Q}$ tensor[3] for nonlinear deformations. This value gives the correct exponential scaling of relaxation times with molecular mass.[10,11]

Doi and Edwards [ref 3, section 6.4.1] calculate that the probability a primitive chain has a contour length z in equilibrium is given by

$$\Psi(z) \propto \exp\left[-\frac{3}{2Nb^2}(z-\bar{z})^2\right] \tag{4}$$

This has its maximum at $\bar{z}$, which by eq 2 is equal to Nb^2/a. The associated free energy is

$$F = -kT\log\Psi = \frac{3kT}{2Nb^2}(z-\bar{z})^2 \tag{5}$$

This free energy can be thought of as arising from a force acting on the branch points to maintain the primitive path contour length z. The force may be written

$$f_e(z/\bar{z}) = \frac{\partial F}{\partial z} = f_0\left(\frac{z}{\bar{z}} - 1\right) \tag{6}$$

with $f_0 = 3kT/a$ and $z/\bar{z}$ the stretch ratio of the primitive path. The force can be further decomposed into an entropic tension along the primitive path $f_0 z/\bar{z}$ and a tension f_0 from the free end. The free end tension f_0 arises because the free end may explore any direction in 3-space whereas the rest of the polymer chain is confined to lie along its tube. Thus, the primitive path is equivalent to a Hookean spring.

In a flow the orientation of the primitive chain is renewed by the free end exploring new conformations. There is a competition between the aligning effect of the flow, given by velocity gradient $\mathbf{K} = (\nabla\mathbf{v})^T$, and the relaxation dynamics from the free ends. Once the free end has passed a point on the primitive path a single time, the orientation of the primitive path up to that point will become isotropic. Therefore, the orientational relaxation time for a point on the primitive chain is the mean first passage time for a branch point to reach that point.[10]

1.2. Cayley Tree Topology. The particular molecular topology we shall consider is that of a Cayley tree,[6,8] as shown in Figure 1. In our highly symmetric topology we can divide all the sections of chain in the molecule into a number of layers. All chain segments in each layer have the same mass and are connected to a fixed number of other chains. We will number the layers from the center of the molecule to the free ends, so that the outermost arms form layer n and the layer nearest the center is 1. Arc coordinates x_i are defined from the centermost end of each segment toward the free end,

so that $x_i = 0$ at the innermost end of each segment in layer i and $x_i = 1$ at the outermost end. (Thus, $x_1 = 0$ is the center of the molecule.) For convenience, another coordinate y runs from the center to the free end so that, in layer i, $y = (i - 1) + x_i$. The number of arms in layer i, attached to each branch point at $y = i - 1$, is denoted q_i. For a Cayley tree $q_1 > 2$, so that there is a branch point in the center of the molecule and reptation is inhibited.

The molecular mass of each polymer chain segment is divided by the entanglement mass, M_e, to give dimensionless path lengths. Thus, $s_i = M_i/M_e$ is the dimensionless length of all arms in layer i. (We will reserve s_i for the path length prior to any dilution scaling from relaxation of the entanglement network.) In each layer the total number of arms is $n_i = \prod_{j=1}^{i} q_j$, and so the total molecular mass of the molecule is $M_T = \sum_i n_i M_i$. We can then define the mass, or volume, fraction for each layer as $\phi_i = n_i M_i / M_T$. As the relaxation progresses through the layers, from the free ends inward, the fraction of unrelaxed polymer chain decreases. Thus, we choose to define

$$u_i = u_{i-1} + \phi_i \quad \text{with } u_0 = 0$$

as the fraction of unrelaxed material, when the relaxation has reached the branch point at $y = i$. This notation provides a framework in which we can calculate relaxation times using a generalization of the Milner−McLeish theory[1] for star polymers.

The Cayley tree topology is specified by the values of q_i and s_i, for $i = 1, ..., n$. In addition, we only need to specify two-dimensional parameters: the plateau modulus, G_0, and the Rouse time of an entanglement segment, τ_e. These two parameters are dependent on the chemical structure of the polymer and the temperature. In tube model theories such as the one presented here, topology governs the qualitative nature of the rheology, whereas quantitatively we take account of the chemistry (and temperature, concentration, etc.) via G_0 and τ_e. Note that these two parameters are independent of the topology and may be fixed by experiments on, say, linear polymers of the same chemistry. Therefore, this theory is topological in the sense that our key parameters are q_i and s_i.

All calculations in this paper are conducted on a three-level Cayley tree with a carefully chosen parameter set. A three-level tree is the minimum structure required to find molecular segments that are not joined directly to segments with free ends. The presence of such segments introduces new physics not seen in the simpler star and pom-pom architectures. On the other hand, the three-level structure will capture all the necessary coupling between segments that may be found in higher order branching structures. Since in typical branched polymers the branch point functionality is three, we set $q = (3, 2, 2)$. The choice of $q_1 = 3$ inhibits reptation and simplifies the model to starlike relaxation modes only. However, reptation in the case of $q_1 = 2$ may be included simply by generalizing the recent work on H-polymers.[2] With the Cayley tree topology, the starlike relaxation may give very long relaxation times due to an exponential dependence on the path length. Thus, we select path lengths short enough to give experimentally accessible rheological features, yet long enough for the segments to be properly entangled. Finally, so that no single segment dominates the rheology we set $s = (12, 6, 3)$, giving equal mass fractions in each segment.

The proposed three-level branching structure will capture features present in all well-entangled treelike polymers. One caveat is that not all polymers will remain well-entangled as they relax. Calculations presented here assume that entanglements restrict the dynamics throughout the relaxation. The calculations reveal how entanglements couple the dynamics of the tree segments. Such coupling must also be present in more general branching structures.

2. Branch Point Diffusion

Orientation of the primitive chain is lost by free ends exploring the primitive path, but for inner segments this requires the branch point to move along the primitive path. So in branched polymers the branch points slow the chain dynamics and dominate the stress relaxation process. Similarly stretch is relaxed by the branch points at the ends of the primitive chain moving toward each other. Consequently, the stress relaxation dynamics arise from diffusion of branch points along the primitive path.

Cooperative motion of all outer arms is required for a branch point to move. Consider, for example, branch points immediately next to the free ends in our hierarchy. These branch points are equivalent to the branch points in an H-, or pom-pom, polymer. The tube pins these branch points at a fixed position until the free ends diffuse down to the branch point. Free end diffusion releases the arms from their tube, which allows the branch point to make a diffusive hop.[12] Rather than requiring simultaneous retraction of all free ends, it has been shown that there is an approximately linear dependence of the branch point hopping time on the number of free ends.[2,9,12] The linear dependence may be pictured as consecutive retraction of all the arms giving a full diffusive step. The branch point hopping idea generalizes to inner segments in the Cayley tree hierarchy. For relaxation to progress beyond branch point i requires motion of all $p_i = \prod_{j=1+1}^{n} q_j$ free ends. Hierarchically, this is equivalent to retraction of the outer $(i + 1)$ branch points up to branch point i.

Several authors have considered the branch point diffusion coefficient in more detail. A full expression for the dependence of the diffusion coefficient on the number of arms in a lattice is given by Rubinstein,[13] but the linear approximation is valid for all values used here. Marrucci,[14] and also Klein,[15] consider an additional stress relaxation mechanism that is important for three-arm star polymers. The idea is that the branch point can diffuse directly, dragging the connected arms into the tube. For the three-arm case, the entropic penalty for this relaxation mode is the same as the penalty for arm retraction. Thus, one might expect that the effective branch point diffusion constant is doubled. However, given the current uncertainty[16] over the prefactor in eq 7, any such a change may be absorbed into that value. Therefore, we neglect these complications and use linearity in the number of arms.

At each level in the hierarchy, the entanglement network (that forms the tube) consists only of the chains that have yet to relax. This leads to a dilution effect in which the tube diameter, a, becomes larger as outer segments in the hierarchy relax. We will return to this in more detail in the following section. Here we simply note that the step size for the diffusive hops, which is

simply the tube diameter, is a function of the unrelaxed volume fraction at the current branch point, $a = a(u_i)$. [In fact, experiments on well-characterized H and comb structures indicate the presence of an $O(1)$ prefactor to the hopping distance that is <1.] Thus, branch point i makes a diffusive hop of size $a(u_i)$ in time $q_{i+1}\tau_{i+1}(0)$. The diffusion coefficient of the branch point at $y = i$ is therefore given by

$$D_i = \frac{a^2(u_i)}{6q_{i+1}\tau_{i+1}(0)} \tag{7}$$

A factor of 6 arises because the diffusion may take place in 3-dimensional space, regardless of our concern only for diffusion along the one-dimensional primitive path. This accounts for the observation that only a fraction of the moves in 3-dimensions will be favorable to stress relaxation, i.e., "down the tube". The diffusion constant of the branch point also specifies the friction coefficient of the branch point ζ_i via the Einstein relation:

$$\zeta_i = \frac{kT}{D_i} \tag{8}$$

The relaxation of polymer chains in the outermost segment, n, is different from other segments because there is no branch point at the end. However, except at early times where Rouse dynamics of all the chain Rouse modes are important, we can assume that the free end carries all the friction.[1] The diffusion coefficient, D_n, of the free end is twice the Rouse diffusion coefficient of the whole arm. This is because the velocity of the free end of a uniformly retracting arm is twice the average curvilinear velocity. Therefore, to give the same drag force, the sum of monomeric drag is halved, and via the Einstein relation (8), the diffusion constant doubled. Thus

$$D_n = 2kT/N_n\zeta_0 \tag{9}$$

With this idea, outermost arms follow the same diffusion process as inner arms, with an effective branch point diffusion constant D_n at the free end.

Now that the branch point diffusion coefficients have been found, the remaining task is to obtain an equation of motion for the position of each branch point along the primitive path. Segments from layer i are treated independently of segments in other layers, and the results combined after the first passage time have been calculated. Treating each layer separately is valid because of the exponential separation of time scales in the relaxation hierarchy.[6] As the relaxation progresses from high to low y, the branch point at $y = i - 1$ will be pinned by the entanglement network until the relaxation reaches $y = i - 1$. Noting that branch points are massless particles, we consider one-dimensional diffusion of massless particles in the potential given by eq 5. We follow Doi and Edwards,[3] McLeish's original work on H-polymers,[12] and the Milner−McLeish treatment of star polymers.[1]

Diffusion in a potential is governed in general by the Smoluchowski equation. In our case we define z_i as the real distance along the primitive path measured from the branch point at $y = i - 1$ out to the branch point at $y = i$. This gives the primitive chain length for all segments in layer i. Similarly, z_i' is the distance to a general point on the primitive path, measured from

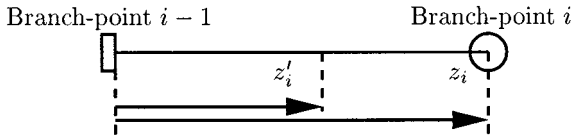

Figure 2. Coordinates used to consider branch point diffusion. Branch point i diffuses toward branch point $i - 1$, which is trapped by the entanglement network. The chain length in this layer, i, is $z_i(t)$. In equilibrium $z_i(t) = \bar{z}_i$. Coordinate z_i' refers to a general point on the primitive path.

branch point $i - 1$. These coordinates are illustrated in Figure 2. The Smoluchowski equation arises from the continuity equation. Let $\Psi_i(z_i,t)$ be the probability distribution for the position of branch point i, z_i, at time t. Then the continuity equation gives

$$\frac{\partial \Psi_i}{\partial t} + \frac{\partial}{\partial z_i}(v_i \Psi_i) = 0 \tag{10}$$

where v_i is the velocity of branch point i relative to branch point $i - 1$. This velocity is composed of the external flow, v_f, together with an additional velocity arising from the entropic forces on the particle. Thus

$$v_i = v_f(z_i,t) + \frac{1}{\zeta_i}\left(-f_e(z_i/\bar{z}_i) + \frac{\partial}{\partial z_i}(kT \log \Psi_i)\right) \tag{11}$$

The external flow gives rise to an affine primitive chain velocity, relative to the center of the molecule, of[3]

$$v_a(z,t) = \mathbf{K}: \int_0^z dz'\, \mathbf{u}(z',t)\, \mathbf{u}(z',t) \tag{12}$$

at distance z along the primitive path from the center of the molecule. Averaging over the orientation distribution and taking account of the multiple segments, one obtains

$$v_a = \mathbf{K}(t): \sum_{j=1}^{i} \int_0^{z_j} dz_j'\, \mathbf{S}_j(z_j',t) \tag{13}$$

for the velocity of branch point i due to affine deformation. Then along the primitive path, the flow velocity of branch point i relative to branch point $i - 1$ is $v_f(z_i) = v_a - \dot{z}_{i-1}$. Here $\mathbf{S} = \langle \mathbf{uu} \rangle$ is the chain orientation tensor, averaged over the distribution for $\mathbf{u}$. Strictly this term should not be preaveraged over $\mathbf{u}$, since diffusion along the primitive path does affect the orientation of the chain. Later, however, we will neglect this term for relaxation of the orientation and include it only for chain stretching. Using this expression gives the Smoluchowski equation for diffusion of the branch point along the primitive path:

$$\frac{\partial \Psi_i}{\partial t} - \frac{\partial}{\partial z_i}\left(\mathbf{K}(t): \sum_{j=1}^{i} \int_0^{z_j} dz_j'\, \mathbf{S}_j(z_j',t)\Psi_i - \dot{z}_{i-1}\Psi_i + \frac{1}{\zeta_i} f_e(z_i/\bar{z}_i)\Psi_i - \frac{kT}{\zeta_i}\frac{\partial \Psi_i}{\partial z_i}\right) = 0 \tag{14}$$

Note that, to write the Smoluchowski equation in level i only, we need to preaverage over all configurations for $j < i$.

Equation 14 governs the diffusion of branch points along the primitive path. As we have described, this can be used to calculate the stress relaxation dynamics.

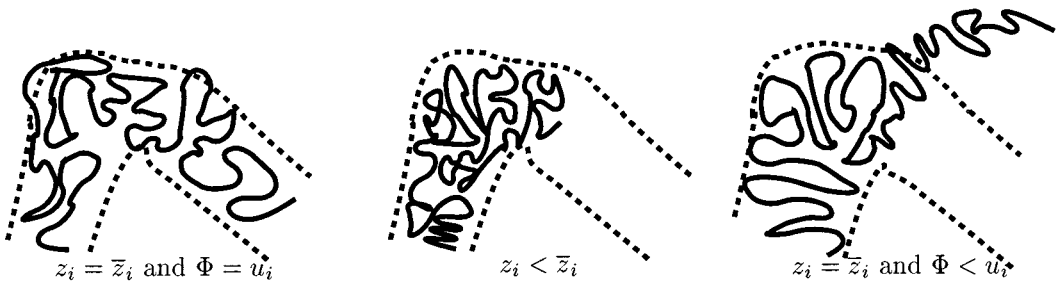

Figure 3. Starlike retraction process, with dynamic dilution. Chains escape from their tube by compressing the spring. This relaxation dynamically reduces the entangled volume fraction Φ.

First we consider the linear rheology, using the equation to derive relaxation times for each layer in the molecule separately. The dilution effect mentioned in this section is significant; it dynamically increases the step length as relaxation progresses.

3. Relaxation Times for Linear Rheology

Relaxation times can be calculated using the results for diffusion along the primitive path. Since the diffusion occurs against the spring force, f_e, relaxing motion has an energy cost associated with compression of the molecular spring. Entropically, to escape from its tube, the primitive chain must shorten. The energy arises because fewer configurations are compatible with a chain contour length shorter than in equilibrium. Relaxation times scale exponentially with this potential,[10] and dimensions are given by $\bar{z}_i^2/D_i$. Exact prefactors are given by solving the Smoluchowski equation from section 2, following the technique used for star polymers by Milner and McLeish.[1] Also, following Milner and McLeish,[1] unentangled dynamics are included for the first entanglement length closest to the free end of each segment. Expressions for the early (unentangled) and late (entangled) relaxation times are combined to give a single relaxation time for each point along the primitive chain.

First we consider relaxation from small-amplitude or low-rate deformations. This gives a spectrum of relaxation times that give the linear rheological spectra G' and G''. In linear rheology, all polymers start at their equilibrium length, $\bar{z}_i$. Also, the flow velocity, v_f, is neglected in the Smoluchowski equation. Only the orientation of the primitive chains is significant, and this is relaxed by the segments fluctuating about their equilibrium length. These fluctuations are described by the equation for branch point diffusion, which for linear rheology reduces to

$$\frac{\partial \Psi_i}{\partial t} - \frac{\partial}{\partial z_i}\left(\frac{1}{\zeta_i} f_e(z_i/\bar{z}_i)\Psi_i - \frac{kT}{\zeta_i}\frac{\partial \Psi_i}{\partial z_i}\right) = 0 \qquad (15)$$

for branch point i. This equation may be solved for the first passage time of the branch point to any point along the primitive path. The first passage time derived in this section is identified as the orientational relaxation time[1] of the associated segment of the primitive path.

The fluctuations in the position of the branch point compress the spring of force f_e. Equivalently, the spring potential $U_i(z_i)$ may be defined. For the Hookean spring the potential U_i is quadratic in z_i; however, the important dilution effect renormalizes this potential. The idea, known as "dynamic dilution",[11] is illustrated in Figure 3. As the boundary between relaxed and unrelaxed portions of the chain moves toward the center of the molecule, the current relaxation time increases exponentially. Therefore, on the time scale where the current portion of chain starts to relax, all parts of the molecule closer to the free end fluctuate rapidly. These rapidly fluctuating parts of the molecule cannot constrain the currently relaxing chain. Thus, the entanglement spacing or chain step length a increases as the relaxation progresses toward the center of the molecule. Incorporating these effects, as detailed in Appendix A, gives the energy barrier to relaxing fluctuations as $U_i(z_i) = \nu_i'(z_i/\bar{z}_i)s_i kT$, with

$$\nu_i'(x_i) = \frac{\nu}{\beta(\beta+1)\phi_i^2}(u_i^{\beta+1} - (u_{i-1} + x_i\phi_i)^\beta(u_i + \beta\phi_i(1 - x_i))) \qquad (16)$$

Scaling parameters $\alpha = {}^4/_3$ and $\beta = \alpha + 1$ quantify the dilution scaling.[17] The tube diameter scales with the unrelaxed fraction in each layer as $a(u_i) = a_0 u_i^{-\alpha/2}$.

Around the first entanglement spacing of each segment, motion is not restricted by the spring potential. This part of each segment relaxes first by free diffusion. Therefore, following Milner and McLeish,[1] we separate the relaxation process into two regimes: an early-time free diffusion and a late-time activated diffusion. The free diffusion is the Rouse-like motion that occurs before tube constraints are felt. At later times the spring potential, derived above, gives an energy barrier to the diffusion process, and we use dynamic-dilution theory together with the Smoluchowski equation.

Defining $\tau_i(x_i)$ as the relaxation time of the chain at arc coordinate x_i, we work with each layer separately; all segments in each layer are identical. The topology gives rise to a hierarchy of relaxation. Inner segments are trapped by the tube at their branch points until the outer segments have relaxed. After waiting a time $\tau_{i+1}(0)$ segment i starts to relax. Relaxation occurs first in the free diffusion time $\tau_{E,i}(x_i)$ and then by dynamic dilution, $\tau_{L,i}(x_i)$. A crossover formula is used to combine early and late time results[1] for each segment. Since we have to wait a time $\tau_{i+1}(0)$ before segment i can start to relax, the overall relaxation time is

$$\tau_i(x_i) = \tau_{i+1}(0) + \frac{\tau_{E,i}(x_i)e^{U_i(x_i)/kT}}{1 + \frac{\tau_{E,i}(x_i)}{\tau_{L,i}(x_i)}e^{U_i(x_i)/kT}} \qquad (17)$$

This defines a continuous relaxation time $\tau(y)$, which is a decreasing function of y. Below we calculate the early time result and then the late time result for a segment i.

Dimensionally, the relaxation times will scale as $\bar{z}_i^2/D_i$, which is evaluated as follows. The equilibrium tube contour length of segments in layer i, when the relaxation has reached the branch point at $y = i + 1$, is $\bar{z}_i(u_i) = (\nu/3)s_i a_0 u_i^{\alpha/2}$. For inner segments with $i < n$, the diffusion coefficient is given by eq 7, so

$$\frac{\bar{z}_i^2}{D_i} = \left(\frac{\nu}{3}s_i u_i^{\alpha}\right)^2 6q_{i+1}\tau_{i+1}(0) = \frac{75}{8}(s_i u_i^{\alpha})^2 q_{i+1}\tau_{i+1}(0) \quad (18)$$

This specifies the prefactor for the more detailed calculation below. The prefactor for the relaxation time of the outermost segments is slightly different due to the spread of drag throughout the segment. Taking the effective branch point diffusion constant (9), together with the definition of τ_e, gives a different scaling in the dimensionless path length:

$$\frac{\bar{z}_n^2}{D_n} = \frac{\nu}{2}\pi^2 s_n^3 \tau_e \quad (19)$$

With inner segments ($i < n$) and early-time branch point motion, the friction blob at the branch point dominates the dynamics. Free one-dimensional diffusion of the branch point, from 1 to x_i (a distance of $(1 - x_i)\cdot\bar{z}_i$)), gives a mean passage time

$$\tau_{E,i}(x_i) = ((1 - x_i)\bar{z}_i)^2/2D_i$$
$$= \frac{75}{16}(s_i u_i^{\alpha})^2 q_{i+1}\tau_{i+1}(0)(1 - x_i)^2 \quad (20)$$

Free diffusion follows a different form for segments in the outermost layer. For $i = n$ we use a Rouse scaling result, following the theory for star polymers:[1]

$$\tau_{E,n}(x_n) = \left(\frac{15}{16}\right)^2 \pi^3 s_n^4 (1 - x_n)^4 \tau_e \quad (21)$$

(This is also important for linear polymers.[18]) Here, the mean passage time is used as the rheologically relevant statistic since the mean first passage time is formally infinite, unless finite extensibility of the primitive path is included in the model.

After waiting a time $\tau_{i+1}(0)$ the segment i can start to relax, and apart from the first entanglement spacing which relaxes rapidly as above, the spring potential is significant. On this time scale all segments $j > i$ have relaxed and simply give the branch point drag. Thus, the Smoluchowski equation (15) gives the probability distribution for the branch point. We consider motion of the branch point along the primitive path, which we call retraction.

For late time, entangled dynamics we calculate the mean first passage time from eq 15. Following ref 1, the first-passage time problem for a single particle is equivalent to having a steady current, J, of diffusing particles:

$$J = \frac{1}{\zeta_i} f_e(z_i'/\bar{z}_i)\Psi_i(z_i',t) - D_i \frac{\partial \Psi_i}{\partial z_i'}(z_i',t) \quad (22)$$

and the mean first-passage time to reach z_i starting at $\bar{z}_i$ is

$$\bar{\tau}(z_i) = J^{-1}\int_{\bar{z}_i}^{z_i} dz_i'\, \Psi_i(z_i') \quad (23)$$

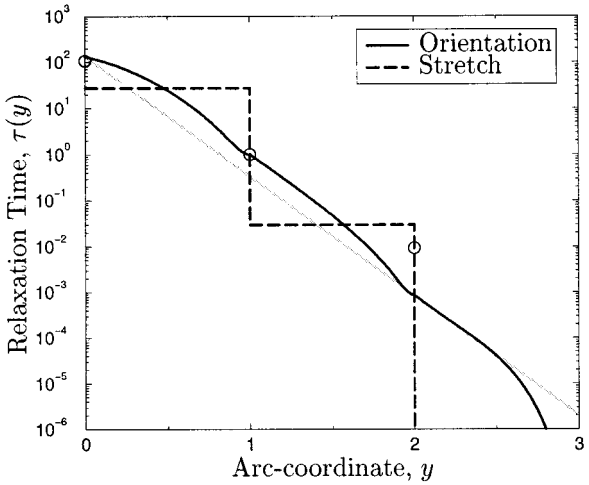

Figure 4. Hierarchy of relaxation times for Cayley tree polymer with $q = (3, 2, 2)$, $s = (12, 6, 3)$. Dimensions are chosen so that $\tau(1) = 1$. The gray curve shows a single exponential, $\tau(0)e^{-cy}$ with $c = 6.0$, for comparison. Stretch relaxation times are defined by eq 40. The circles show results from the simpler calculation of McLeish,[12] again with $\tau(1) = 1$.

Equation 22 can be solved for Ψ by multiplying by the integrating factor

$$I(z_i') = \exp\left[\frac{1}{kT}\int_{\bar{z}_i}^{z_i'} dz_i''\, f_e(z_i''/\bar{z}_i)\right] = \exp[U_i(z_i'/\bar{z}_i)/kT] \quad (24)$$

Taking care with dilution scaling gives the potential U_i (see Appendix A), identified as a free energy barrier to retraction, modified by dynamic dilution. Multiplying (22) by $I(z_i')$ and integrating gives

$$\Psi(z_i) = \frac{J}{D} I(z_i)^{-1}\int_{z_i}^{\infty} dz_i'\, I(z_i') \quad (25)$$

The limit ∞ includes the possibility of branch point diffusion stretching chains; there is no reflecting boundary at $z_i = \bar{z}_i$. Integrating again, from the initial condition $\bar{z}_i$, using (23) gives the first passage time. Noting that $z_i = \bar{z}_i x_i$ gives the relaxation time for the tube at x_i (the dimensionless coordinate introduced in section 1.2):

$$\tau_{L,i}(x_i) = \frac{\bar{z}_i^2}{D_i}\int_1^{x_i} dx'\, e^{U_i(x')/kT}\int_{\infty}^{x'} dx''\, e^{-U_i(x'')/kT} \quad (26)$$

These integrals may be computed numerically or approximated by following Milner and McLeish.[1] Combining this first passage time with the early time result ((20) or (21)) in the formula (17) gives the relaxation time for any point y along the polymer chain.

Relaxation times for any entangled Cayley tree polymer may be calculated using the expressions derived in this section. For the $s = (12, 6, 3)$, $q = (3, 2, 2)$ polymer, the results are shown in Figure 4. However, the validity of the entangled dynamics, which we assume, should be checked. The simplest test, that the dilution-scaled path lengths $s_i u_i^{\alpha}$ remain greater than unity,[6] does hold in this case. However, the *rate* of relaxation must also be checked. Using a condition proposed by Milner et al.,[19] that the rate of tube dilation should always less than the rate of retraction, in Appendix B we find that entanglements remain important for this particular choice of polymer. The time scale

generally follows a single-exponential shape in the dimensionless variable y, with the renormalized spring potential giving hump shapes for each layer. This is consistent with theoretical and experimental work on H-polymers[2] where the "humps" from each segment become more pronounced in the $G''(\omega)$ curve. The curve in Figure 4 can be used, when interpreting such rheological data, to identify which parts of the molecule are active at different times or frequencies.

McLeish[12] calculated the relaxation times for entangled tree polymers using a simplified model for dilution effects. He calculated the terminal relaxation time for each layer in the tree, with an exponential scaling in the diluted path length. The dynamic dilution scaling of Ball and McLeish[11] was not included, however. Instead of the variable ν' (eq 16), changing at each stage in the relaxation, McLeish[12] used a constant value for each layer. In contrast, our calculation includes the full effect of dynamic dilution. For comparison, we applied McLeish's earlier calculation to the $s = (12,6,3)$, $q = (3, 2, 2)$ polymer. We used an effective ν' of unity and used the diluted path length $s\Phi$ to calculate the relaxation time following McLeish. The results, included in Figure 4, show that the earlier model underestimates the difference in dilution between layers 1 and 2 in the tree.

The relaxation time may be transformed into the linear spectra G' and G'', giving predictions for the response to small-amplitude deformations. This is presented in section 5. The relaxation time distribution is also the first ingredient in a description of the orientation dynamics in nonlinear flows. We proceed to derive a constitutive equation for the stress in nonlinear flows in the following section.

4. Nonlinear Transient Stress

Following the work on H-polymers[2] and generalizing the pom-pom equations,[9] we may write a constitutive equation for the stress in a general flow, $\boldsymbol{\sigma}(\mathbf{K},t)$. The stress from each segment depends on a molecular stretch ratio λ_i, defined as $\langle z_i(t)/\bar{z}_i\rangle$, and the orientation tensor given by the second moment of the primitive chain tangent vectors, $\mathbf{S}_i = \langle \mathbf{u}_i\mathbf{u}_i\rangle$. In equilibrium the polymers have a stretch ratio of unity and are oriented isotropically. Flow stretches chains above their equilibrium length and orients them along the flow direction. The chain relaxation dynamics, dominated by branch point diffusion, compete with the flow. The resulting anisotropic stress is the rheological response of the polymer melt and gives an experimental window on the chain dynamics.

The central result of the successful pom-pom model[9] is that orientation and stretch dynamics decouple, with different relaxation times for each. Here we retain this separation by assuming that the probability distributions for stretch and orientation are independent. Clearly this is not generally true, yet it may be a valid approximation at flow rates of interest. We formulate separate differential equations for the stretch and orientation of the polymer chain. Here the different relaxation times arise because the stretch relaxes when the *mean* primitive chain length reduces, yet orientation is lost with the *first passage* of the chain end. Thus, in our picture, for each segment, portions of chain close to the free-end lose orientation faster than stretch, yet portions far from the free end lose stretch first. This separation of orientation and stretch means that the orientational relaxation times are just the relaxation times for linear flows calculated in the previous section.

Another way of seeing that the relaxation time for linear flow is valid for nonlinear flow is given as follows. In nonlinear flow the affine velocity v_a is significant and stretches the chains, yet the linear flow relaxation time assumes initially unstretched chains. We consider the effect of the branch point velocity v_a on orientation relaxing fluctuations in the position of the branch point. In general, the fluctuations occur around the ensemble averaged chain length $\langle z_i\rangle$. Now exponentially varying relaxation times mean that all the contribution to v_a comes from the oriented parts of the chain. Therefore, local to $\langle z_i\rangle$, v_a is approximately constant. In eq 14 the effect is to add a constant force to f_e, shifting the energy minimum to $\langle z_i\rangle$, but not changing the shape of the potential. Therefore, we conclude that the linear flow relaxation time also describes the orientational relaxation in nonlinear flow.

Doi−Edwards' expression for the stress counts the force carried by the chains across a given plane.[3] The force is simply $\mathbf{F}_i(z_i',t) = f_0[(z_i(t)/\bar{z}_i]\mathbf{u}_i(z_i')$ (see section 1), and the number of chains crossing the plane at z_i' is proportional to $\mathbf{u}_i(z_i')\,dz_i'$. In this approach the stresses from each segment are additive. A single value of the stretch ratio is used for each segment by noting that (on time scales above τ_e) the outer segments never stretch ($\lambda_n \equiv 1$) and that the stretch of the other segments rapidly equilibrates between their confining branch points. Using the Colby−Rubinstein scaling argument[17] and the dynamic-dilution idea of widely separated time scales along the chain,[11] one may write

$$\boldsymbol{\sigma}(\mathbf{K},t) = \nu G_0 \sum_{i=1}^{n} \lambda_i^{\,2}(\mathbf{K},t) \int_0^1 dx_i\, \mathbf{S}_i(\mathbf{K},x_i,t)\, \frac{d}{dx_i}\Phi_i(x_i)^{\beta} \quad (27)$$

Essentially, contributions $\lambda^2\mathbf{S}$ are counted from each point along the chain and multiplied by the appropriate dilution factor. Stress scales with the square of the stretch ratio, with one contribution from the force in the chain and one from the chain length. It remains to write expressions for the stretch and orientation of the primitive chain in each segment.

4.1. Orientation. In tube models orientation of the polymer chain is controlled by the tube, which represents the entanglements with other chains. Relative motion between the chain and its entanglements gives rise to the orientation dynamics. The tube is assumed to move affinely with the imposed flow,[3] so that tube segments align along the flow direction. Relaxation toward isotropy occurs by the branch point diffusion process (section 2), allowing chains to escape from their tube. In addition to these competing effects of flow-induced alignment and relaxation from chain dynamics, advection of tube along the polymer chain is also significant for the Cayley tree topology.

In the Cayley tree the relaxation times are exponentially varying along the primitive chain, and this can lead to large gradients in the orientation along the chain. However, motion of tube along the primitive chain can be significant in reducing these gradients. This motion, which we term *tube advection*, is simply the component of the affine tube motion along the primitive chain. Projecting the flow gradient onto the chain means that the along-chain velocity depends on the orientation of the chain. Tube advection means that a particular element of primitive chain is not con-

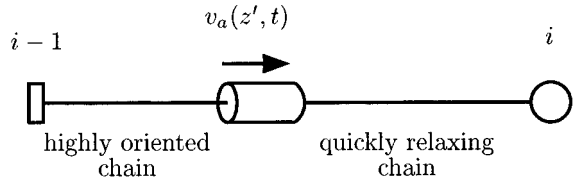

Figure 5. Tube advection: relative motion between the affine tube and relaxing chain orients chain with short relaxation times.

strained by a single tube segment throughout the flow history, and so orientation does not only depend on the local relaxation time. Highly oriented tube from the center of the molecule moves out to parts of the chain with faster relaxation times (Figure 5). Advection did not arise in the pom-pom model for two branch point polymers,[9] because the approximation of a single reptation time was used for the entire length of chain between branch points.

Alignment, by relative tube-chain motion, has been included in earlier theories[8,9] but only at high strain rates. Termed "branch point withdrawal" the physical idea is that beyond a certain local deformation rate, the tube velocity exceeds the local diffusive hopping rate, giving chain alignment.[20] Although this was pictured as occurring primarily at branch points, we recognize that the process occurs along the entire chain. We include the chain alignment effect of branch point withdrawal directly into the orientation equation, using the idea of tube advection. Some effects local to the branch points are still important and will be discussed later in this section.

Doi and Edwards[3] give an integral equation for the orientation of polymer chains $\mathbf{S} = \langle \mathbf{uu} \rangle$. However, advection of tube along the chain may be more readily incorporated into a differential equation. Therefore, we develop the differential pom-pom orientation equation.[9] This has been shown to produce functional forms close to the full Doi−Edwards results. Allowing the orientation to vary along the chain, we denote the second moment of the primitive chain tangent vectors, at arc coordinate x_i, by $\mathbf{S}_i(x_i,t)$. We assume this is identical for all segments at x_i in layer i. In generalizing the equation, we make a careful distinction between the coordinates z_i', which represent a real distance along the primitive path, and the dimensionless variable x_i. As soon as an along-chain dependence of local orientation and stretch is introduced, total derivatives must contain an extra term for movement along the chain. Such a term is used by Marrucci[21] to calculate the tube survival probability for fixed-length linear polymers; however, we include the dynamics directly into a differential equation for the orientation. Recognizing that the flow causes relative motion between the chain and its constraining tube is equivalent to formulating Doi−Edwards' model without the "independent alignment approximation".[3] Thus, we recognize that the advection term may be significant, not only for reversing flows[3] and effects which depend on the first normal stress difference[22] as found in linear polymers but also in forward flows.

Starting from the differential form of the pom-pom orientation equation, we derive a local orientation equation valid for the Cayley tree topology. At each point along the chain, we consider a small section of chain deformed by the flow and relaxing with the relaxation time of that point. Following ref 9, we calculate the unit trace orientation tensors, $\mathbf{S}_i(x_i,t)$, by first introducing the nonnormalized tensors $\mathbf{A}$ obeying the following equation. Using real distances along the primitive path, we may write[9]

$$\frac{\mathrm{D}}{\mathrm{D}t'}\mathbf{A}(z',t') - \mathbf{K}\cdot\mathbf{A}(z',t') - \mathbf{A}(z',t')\cdot\mathbf{K}^{\mathrm{T}} = -\frac{1}{\tau(z')}(\mathbf{A}(z',t') - \mathbf{I}) \quad (28)$$

where $\mathbf{A}(z',t')$ represents the orientation of the tube at distance z' from the center of the molecule and time t'. The unit-trace tensor, $\mathbf{S}$, which is the second moment of the unit tube tangent vectors is then given by

$$\mathbf{S}(z',t') = \frac{\mathbf{A}(z',t')}{\mathrm{Tr}\ \mathbf{A}(z',t')} \quad (29)$$

Now allowing for advection of tube along the chain, we note that the total derivative must contain a term in the variable z'. Making this explicit, we make the substitution

$$\frac{\mathrm{D}}{\mathrm{D}t'} = \frac{D}{Dt'} + v_{\mathrm{a}}\frac{\partial}{\partial z'} \quad (30)$$

with v_{a} given by eq 12 averaged over the distribution of $\mathbf{u}$. Now (D/Dt') is the usual material derivative in macroscopic 3-space. The additional velocity along the mesoscale primitive path recognizes that the tube always deforms affinely with the imposed flow, whereas the primitive chain does not.

Boundaries between segments are more easily handled using the dimensionless coordinates x_i, so we transform eq 28. Variables (z',t') are replaced by (x_i,t), with $t' = t$. Noting that the real chain length, from branch point $i-1$ to i, is $z_i = \lambda_i\bar{z}_i$ gives the mapping between real distances and fractional distances along the primitive path $z_i' = x_i\lambda_i\bar{z}_i$, and so the distance from the molecular center is

$$z' = \sum_{j=1}^{i-1}\lambda_j\bar{z}_j + x_i\lambda_i\bar{z}_i \quad (31)$$

Therefore, we see that $\partial/\partial z_i'$ at constant t' is $(1/\bar{z}_i\lambda)(\partial/\partial x_i)$. Finally, transforming the time derivative $[D/Dt' = (\partial t/\partial t')(D/Dt) + (\partial x_i/\partial t')(\partial/\partial x_i)]$ gives the orientation equation which we solve in our model:

$$\frac{D}{Dt}\mathbf{A}_i(x_i,t) = \mathbf{K}\cdot\mathbf{A}_i(x_i,t) + \mathbf{A}_i(x_i,t)\cdot\mathbf{K}^{\mathrm{T}} - \frac{1}{\tau_i(x_i)}(\mathbf{A}_i(x_i,t) - \mathbf{I}) - u_i(x_i,t)\frac{\partial}{\partial x_i}\mathbf{A}_i(x_i,t) \quad (32)$$

with

$$u_i = \frac{v_{\mathrm{a}}}{\lambda_i\bar{z}_i} = \sum_{j=1}^{i-1}\frac{\lambda_j s_j}{\lambda_i s_i}\mathbf{K}:\ \int_0^1 \mathrm{d}x_j'\ \mathbf{S}_j(x_j',t) + \mathbf{K}:\int_0^{x_i}\mathrm{d}x_i'\ \mathbf{S}_i(x_i'_i,t) - x_i\frac{\dot{\lambda}_i}{\lambda_i} - \sum_{j=1}^{i-1}\frac{\dot{\lambda}_j s_j}{\lambda_j s_j} \quad (33)$$

We identify u_i as the relative velocity between the affinely deforming tube and the stretch relaxing chain at x_i. The boundary conditions for eq 32 are

$$\mathbf{A}_i(1,t) = \mathbf{A}_{i+1}(0,t) \tag{34}$$

$$\mathbf{A}_n(1,t) = \mathbf{I}\ \forall t \tag{35}$$

by continuity and noting that motion of the free end creates new tube isotropically.

This equation is a first-order hyperbolic PDE, with nonlocal dependence of the velocity $u(y)$ on the solution $\mathbf{A}$ and may be solved via the method of characteristics.[23] The characteristic curves of the PDE are given by

$$\frac{\mathrm{d}y}{\mathrm{d}t} = u(y,t) \tag{36}$$

and along these curves

$$\frac{\mathrm{d}\mathbf{A}}{\mathrm{d}t} = \mathbf{K}\cdot\mathbf{A}(t) + \mathbf{A}(t)\cdot\mathbf{K}^{\mathrm{T}} - \frac{1}{\tau(y)}(\mathbf{A}(t) - \mathbf{I}) \tag{37}$$

Here $\mathrm{d}y/\mathrm{d}t$ is the velocity of the tube segment at y with respect to the center of the molecule and not relative to the underlying chain. Equations 36 and 37 are solved using a Runge−Kutta routine with second-order accuracy together with linear interpolation between values of y. Calculations were performed with a uniform grid of 10 points for each segment type. (Tests with more grid points showed no variation in the results.) Our chosen approximation to the orientation equation dictates that $\nu = 3$ in the stress equation (27) rather than Doi−Edwards' 15/4. (However, we still use $\nu = 15/4$ in the relaxation times.)

The characteristics of eq 32 intersect whenever $(\partial v_a/\partial z') < 0$. This condition occurs whenever tube moving in a given direction moves faster than the tube immediately ahead of it. Characteristics crossing lead to an unphysical multivalued solution where several different tube segments are occupied by the same piece of polymer chain. This occurs because tube is being shrunk relative to the polymer chain. Unlike classical shock formation, in our system the condition is typically true everywhere or nowhere along the chain, so the breakdown occurs everywhere simultaneously. The cure to this problem is to recognize that the tube is not a rigid entity and does not exist on length scales less than the spacing between entanglements, a. Thus, tube curvature on length scales less than an entanglement spacing must be destroyed by averaging $\mathbf{A}$ over its neighboring values, at a rate given by their advection velocity. Therefore, there should be an additional term $a^2|(\partial v_a/\partial z')|(\partial^2\mathbf{A}/\partial z'^2)$ in the dimensional coordinates. This diffusive term is sufficient to ensure that $\partial v_a/\partial z' > 0$. In a forward flow $\partial v_a/\partial z' = \mathbf{K}:\mathbf{S}$ is always positive; however, if the flow direction reverses, it will become negative for a time of order $\tau(z')$. In this paper we discuss only simple flows and therefore neglect the tube-averaging term, which we leave to future work.

The nonlinear PDE reduces to give a linear solution in the rate of strain for the outermost segment n. Since the relaxation times in this segments are so small, we use the Newtonian limit $\mathbf{S}_n(x_n) = {}^1/_3\mathbf{I} + (\tau(x_n)/3)(\mathbf{K} + \mathbf{K}^{\mathrm{T}})$. However, for inner segments under nonlinear flow the full PDE is solved. To give predictions for the stress, stretching of the polymer chain segments must also be included.

4.2. Mean Stretch. Stretch is the other key variable in the nonlinear rheology of branched polymers. Extension hardening is due entirely to stretching of polymer chains magnifying the stress in the melt. The stretching

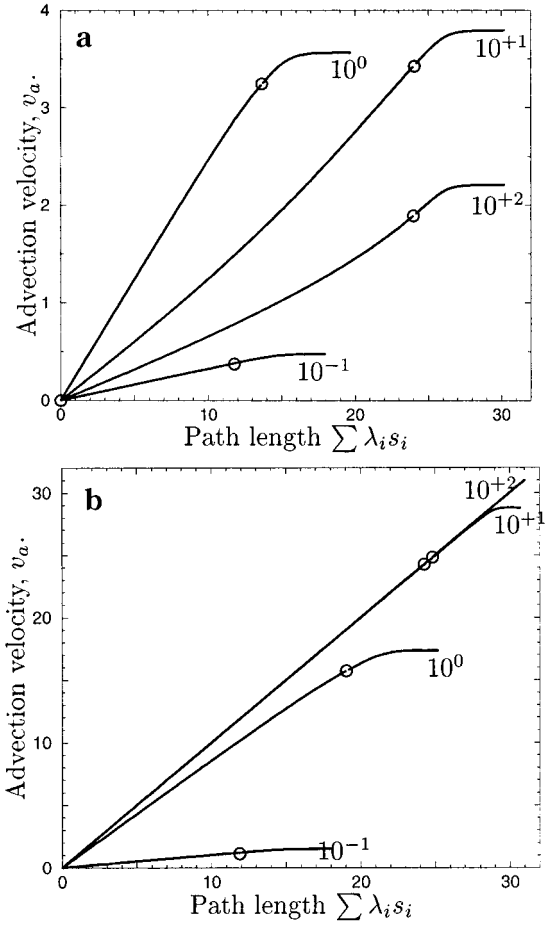

Figure 6. Advection velocity for $q = (3, 2, 2)$, $s = (12, 6, 3)$ polymer in (a) simple shear flow and (b) uniaxial extension. The rate is $\tau(1)^{-1}$, and only the inner two layers are shown. The circles on each curve represents the boundary between layer 1 and layer 2. Curves are labeled by the time, in units with $\tau(1) = 1$.

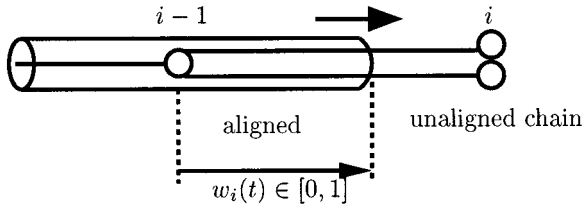

Figure 7. Branch point withdrawal: only unaligned chains contribute to the branch point drag for stretch dynamics. A quantitative measure for branch point withdrawal, $w_i(t)$, is introduced in Appendix C.

arises through flow-induced separation of branch points, competing against the entropic spring force from the polymer chain. The separating force depends in turn on the effective drag on the branch points, but this is itself limited by an important coupling to the flow, termed "branch point withdrawal", when chains at one level are dragged into the tube created by the next deeper level (Figure 7). This causes an exponential reduction in the effective drag of the outer arms on the branch point; its incorporation into pom-pom models of long-chain branched melts strongly suggests that it is responsible for the limiting of extension hardening. In this work we follow ref 9 and assume that stretch is limited by a dynamic reduction in the branch point friction. Chain aligned along the flow direction does not contribute to the branch point friction. As the branch point withdraws

into the inner segment tube, it reduces the length of unaligned chain, reducing the dominant branch point friction. The reduction in branch point friction gives an upper bound to the stretch ratio in each segment, a condition that can also be derived by a force balance at the branch point.[9]

Flow may perturb any of the three segments from their equilibrium length. However, the outermost segment ($i = n$) is not trapped between branch points, and so any stretch will decay on its bare Rouse time scale of $s_n^2\tau_e$, faster than any flow we consider in this work. In the relaxation hierarchy, branch points act as friction blobs dominating the relaxation dynamics of any inner segments (see section 2). This means that stretching of all inner segments ($i < n$) may be significant. In setting up equations for the stretch, we choose coordinates so that the $x_i = 0$ end of the chain segment is our origin and consider the friction blob at the other end relaxing toward it. At first we construct the stretch equation without branch point withdrawal and then modify it in two respects.

The mean stretch λ_i of all segments in layer i may be calculated by balancing the drag force, produced by the flow on the outer branch point, with the spring force in the polymer chain. Multiplying the relative tube chain velocity at branch point i by the friction coefficient gives a drag force

$$F_d = \zeta_i(v_a(z) - \dot{z}) \tag{38}$$

at this branch point. Here $z = \sum_{j\le i} z_j$ is the distance along the primitive path to the branch point, $\dot{z}$ is the material derivative, and the friction coefficient ζ_i is given by eqs 7 and 8. Balancing with f_e from eq 6 gives

$$\frac{D}{Dt}\lambda_i(t) = \frac{1}{\bar{z}_i}\Big(\sum_{j<i}\lambda_j(t)\bar{z}_j\,\mathbf{K}\colon \int_0^1 dx_j\,\mathbf{S}_j(x_j,t) - \dot{\lambda}_j(t)\bar{z}_j\Big) + \lambda_i(t)\mathbf{K}\colon \int_0^1 dx_i\,\mathbf{S}_i(x_i,t) - \frac{1}{\tau_{s,i}}(\lambda_i(t) - 1) \tag{39}$$

with the stretch relaxation time for segment i given by

$$\tau_{s,i} = \frac{\zeta_i\bar{z}_i(u_i)}{3kT/a(u_i)} = 5s_i{u_i}^{\alpha}q_{i+1}\tau_{i+1}(0) \tag{40}$$

The term in parentheses in eq 39 is the relative velocity between the tube and the branch point at $i - 1$. It may be simplified by recursively substituting the equation for the inner segments. This gives

$$\frac{D}{Dt}\lambda_i(t) = \frac{s_{i-1}}{s_i\tau_{s,i-1}}(\lambda_{i-1}(t) - 1) + \lambda_i(t)\mathbf{K}\colon \int_0^1 dx_i\,\mathbf{S}_i(x_i,t) - \frac{1}{\tau_{s,i}}(\lambda_i(t) - 1) \tag{41}$$

which may be solved by the Runge−Kutta method to give the stretch ratio for each segment $i < n$. This equation can also be derived by solving the reduced Smoluchowski equation (14) with the full nonlinear expression for the branch point velocity. Using the Smoluchowski equation requires the assumption that the probability distribution for z_i is a function of preaveraged segment lengths for the other layers.

Implicit in our approach is the recognition that the stretch of inner segments is independent of the stretch of outer segments. This means that there is a coupling outward from the center of the molecule. Stretch relaxation of inner segments gives the inner branch point a finite velocity in the affinely deforming frame. This decreases the velocity of separation of the two branch points, reducing the stretch rate. Inner segments always relax more slowly than outer segments, so they are more highly stretched. This means that the stretch relaxation of inner segments can influence the stretch of outer segments significantly, despite the widely separated relaxation times.

Beyond a critical stretch, the coupling occurs in the opposite direction. In the pom-pom model[9] a coupling from the outer to the inner segments gives a natural limit to the stretch in any segment. As discussed in section 1.1, the requirement of Gaussian statistics in equilibrium gives a Brownian force of $f_0 = (3kT/a)$ on each free end. This force acts to maintain the curvilinear path length of the chain. Applying McLeish and Larson's result to the Cayley tree gives a maximum stretch force for chain segments in layer $(n - 1)$. This maximum stretch force is $q_n f_0$ since each chain in this layer is connected to q_n free ends. The ratio of the maximum force to the equilibrium force f_0 has been called the "priority".[8] The stretch ratio for layer n is therefore constrained by the maximum value q_n.

Priority generalizes in an interesting way to the inner layers in the Cayley tree via the branch point withdrawal mechanism. Chain segments in layer i are each connected to q_{i+1} chains closer to the free end. Each of the chain segments in layer $i + 1$ carry a force $\lambda_{i+1}f_0$, and thus the maximum stretch force for segment i chains is $q_{i+1}\lambda_{i+1}f_0$. We conclude that each segment has a time-dependent priority $p_i(t)$, giving a general condition

$$\lambda_i(t) \le p_i(t) = q_{i+1}\lambda_{i+1}(t) \tag{42}$$

which is the first modification to (41) due to branch point withdrawal. A large step strain, for example, will stretch each segment to its maximum priority $p_i = \prod_{j=i+1}^{n} q_j$. Priority reduction will occur by stretch relaxation of the outer segments. This introduces a time dependence to the work of Bick et al.[8] The maximum stretch condition may also be derived by considering branch point withdrawal explicitly (see Appendix C).

Priority-induced coupling between segments gives interesting effects. Outer segments limit the stretch of inner segments yet by definition are closer to the free end so have much faster relaxation. Therefore, inner segments, which can have the highest priority and contribute most to the extension hardening, can only reach very high stretch ratios at rates and times determined by the outer segment dynamics. Only at very high rates, where outer segments stretch, can inner segments reach their true maximum stretch. This contrasts with experience from using the multimode pom-pom model[4,5] to model LDPE, which assumes that segment priorities are fixed for all strain rates. Matching the extension hardening behavior of LDPE requires very high priorities to be accessed at relatively low rates.

As well as producing a maximum stretch, the branch point withdrawal also aligns the primitive chain and therefore reduces the effective branch point friction. Only the portion of chain unaligned with the flow direction needs to relax before the branch point may make diffusive step. The alignment effect has already been included in the orientation equation as tube

advection. Likewise, the friction reduction gives the maximum stretch condition already stated. However, alignment of chain local to the branch point has been shown to be significant before the maximum stretch is reached.[5] Since branch point withdrawal can be observed in neutron scatting experiments,[2] we derive dynamical equation for a quantitative measure for it in Appendix C. This level of detail is not required for the calculation of stress; however, the consequent reduction of the stretch relaxation time must be included.[5]

Blackwell et al.[5] introduced a modification to the original pom-pom model in which the branch point drag is coupled to the imposed strain. The idea is that alignment of chain around a tube diameter from the branch point reduces the chain length which needs to relax before the branch point can move. Even a reduction of the order of a single tube diameter is significant since the relaxation time scales exponentially with the chain length. As more chain becomes aligned, the maximum stretch is reached, yet this can be delayed by the faster relaxation from the local alignment. We follow ref 5 in modifying the stretch relaxation time to include this effect.

The maximum stretch condition (42) is equivalent to an energy cost for branch point withdrawal which is linear in the withdrawn distance. Reference 5 recognized this potential cannot be linear for local withdrawal and assumed a quadratic potential instead in this regime. For the Cayley tree we can follow ref 5 in linking this potential to the stretch relaxation, with only one change. Here the long-range potential scales with the stretch of outer segments so, by continuity, the local potential must also be linear in $\lambda_{i+1}(t)$. This is consistent with the local physics since stretching outer arms must increase the energy cost for branch point displacement. Resulting changes in the stretch equation (41) follow the form introduced in ref 5. Each occurrence of $\tau_{s,i}$ is replaced by $\tau_{s,i} \exp[-\nu^*_{i+1}(t)(\lambda_i - 1)]$, with variable $\nu^*_i(t) = (6\nu_i'(0))/(5\lambda_i(t)q_i k^*)$. Following ref 5, we assume that the dimensionless strength of the local quadratic potential for branch point withdrawal, $k^* = 0.36$.

The stretch equation (41) with the modified stretch time, orientation equation (32), and the stress equation (27) form the complete constitutive equation for the Cayley tree. This is not a simple generalization of existing constitutive equations. It includes coupling between the various layers in the branching hierarchy. Inner segment stretch relaxation increases the stretch of outer segments. Conversely, outer segments give a time-dependent maximum stretch for the inner segments. Orientation is also coupled between segments by tube advection. In the following section the constitutive equation is used to give predictions for the rheology of a particular Cayley tree.

5. Predictions of the Model

5.1. Linear Response: Dynamic Modulus. In earlier studies[2,12,24] it has been shown that the linear rheological spectrum can reveal information on the topological structure of monodisperse polymers. For example, H-polymers show a characteristic two-hump shape in the loss modulus, G''.[2] Similarly, we expect the three distinct segments in the Cayley tree to give a characteristic shape.

In the linear viscoelastic limit the stress is given by Boltzmann's constitutive equation

$$\boldsymbol{\sigma}(t) = \int_{-\infty}^{t} G(t - t')\, 2\mathbf{D}(t')\, \mathrm{d}t' \tag{43}$$

where $G(t)$ is the relaxation modulus and $\mathbf{D} = {}^1/_2(\nabla\mathbf{v} + \nabla\mathbf{v}^{\mathrm{T}})$ is the rate-of-deformation tensor. Data are usually presented in terms of the storage and loss moduli, G' and G''. These are given by the real and imaginary part of the Fourier transform of $G(t)$.

As expected, the constitutive equation proposed here reduces to eq 43 at low rates. The resulting modulus, G, depends only on the relaxation time. It follows the same form as the H-polymer theory by McLeish et al.[2] and is given by

$$G(t) = G_0 \int_0^n \mathrm{d}y\, \mathrm{e}^{-t/\tau(y)} \frac{\mathrm{d}}{\mathrm{d}y} \Phi(y)^{\beta} \tag{44}$$

The dynamic-dilution scaling[1] is explained in Appendix A.

All calculations is this paper are presented with units $\tau(1) = 1$ and $G_0 = 1$. A time scale of $\tau(1) \approx 1$ s will be required to observe any of the predicted features experimentally, particularly for the nonlinear rheology. This may be achieved in the structure described in section 1.2, for example, by using polyisoprene at around 90 °C.

The zero shear viscosity is found by taking the time integral of the relaxation modulus $G(t)$. It depends on the distribution of relaxation times over the entangled volume fraction:

$$\eta_0 = G_0 \int_0^n \mathrm{d}y\, \tau(y) \frac{\mathrm{d}}{\mathrm{d}y} \Phi(y)^{\beta} \tag{45}$$

Moving toward the center of the molecule, Φ decreases exponentially and τ increases exponentially. The exponential increase of τ, however, is reduced by dynamic dilution. The dilution effect on the zero-shear viscosity is pronounced whenever n and q are greater than three. Polymers with this extreme treelike branching have a high proportion of their mass in the outer layer, and so the zero-shear viscosity depends weakly on the relaxation time of the inner layers. The outer layer, which dominates, has a relaxation time that is a function of the arm length rather than the total molecular weight of the layer. This leads to a surprising result when comparing the zero-shear viscosity of such a branched polymer with a linear polymer of the same total molecular weight. In contrast to the tree-branched structure, the zero-shear viscosity of a linear polymer scales with total molecular weight. Therefore, by concentrating a large proportion of the molecular weight in the outer layers of the branching structure, the zero-shear viscosity of a tree polymer can be made *significantly smaller* than that of a linear polymer with the same molecular weight.

Even in the finely balanced $q = (3, 2, 2)$, $s = (12, 6, 3)$ Cayley tree, this dilution affects the zero-shear viscosity. In our dimensionless units, the zero-shear viscosity is 1.2, which is equivalent to $5 \times 10^6 G_0 \tau_e$. The reptation model[3] can be used to calculate the zero-shear viscosity of a linear polymer with the same molecular weight. We found that it would have the comparable value of $4 \times 10^6 G_0 \tau_e$. Thus, with treelike branching, the viscosity may not be significantly higher than for linear polymers. This is in contrast with star polymers where the zero-shear viscosity is usually much higher than that of the linear polymer.

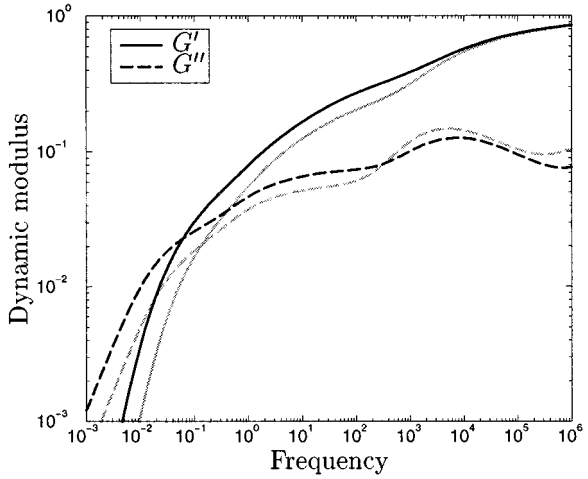

Figure 8. Storage and loss moduli for $q = (3, 2, 2)$, $s = (12, 6, 3)$ polymer. Note the characteristic shape from the three segments. For comparison $q = (3, 2, 3)$, $s = (12, 6, 3)$ is shown in gray.

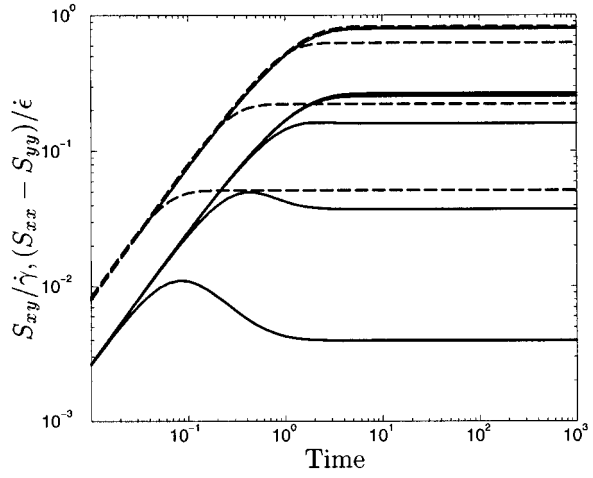

Figure 9. Transient Doi−Edwards form for the orientation in shear (solid) and uniaxial extension (dashed). Calculated using a single relaxation time of unity. Shear rates, $\dot{\gamma}$, and extension rates, $\dot{\epsilon}$, decrease by a factor of 5 from a maximum of 25 for the lowest curves. Units are given in terms of the relaxation time.

Predictions of this theory for the dynamic moduli of the Cayley tree polymer described in section 1.2 are shown in Figure 8. As expected, there are three distinct humps from the three segments in the molecule. The lowest frequency hump is the least pronounced since it represents the slowest relaxation from the innermost segment. At these frequencies the stress carrying entanglement network is at its most dilute. Beyond the high-frequency end of spectrum shown in Figure 8, Rouse motion inside the tube would become dominant. However, this is not included in our calculations.

Changing the molecular weight of the segments would affect the linear rheology in much the same way as in H-polymers. As long as the structure is chosen to maintain the validity of dynamic-dilution, the theory still applies. Typically, increasing the molecular weight of a segment broadens the shoulder in G'' associated with that segment. Changing the arm numbers has a more subtle effect, through changes in the relaxation time and also the dilution from relaxed segments. For example, adding more arms in the outer segment dilutes the effect of inner segments, which reduces the magnitude of G' and G'' at low frequency (Figure 8).

5.2. Nonlinear Rheology. We now examine the behavior of our proposed constitutive equation in start-up flow of both shear and uniaxial extension. We consider a range of deformation rates between 1.6×10^{-3} and 25 $\tau(1)^{-1}$. At these rates the most significant segments are in the inner two layers of the Cayley tree. The general features of branched polymer rheology, such as extension hardening and shear thinning, are produced. However, the coupling between segments, in both stretch and orientation dynamics, gives rise to novel features not observed in the existing pom-pom model for branched polymers.

Generally the orientation should follow the form proposed for linear polymers by Doi and Edwards,[3] with additional features arising from the range of relaxation times and the tube advection. Looking at this result first highlights the distinctive features of Cayley tree polymers. With the independent alignment approximation, the primitive path orientation tensor **S** in Doi−Edwards' theory is given by a history integral. This integral sums the entire history of affine deformation with an exponentially decaying memory function. A geometric tensor $\mathbf{Q}^3$ describes the affine deformation of the primitive chain. The same expression is used to describe the orientation in the original pom-pom model.[9] It is reproduced with a single relaxation time in Figure 9. The orientation is plotted as $S_{xy}/\dot{\gamma}$ in shear and $(S_{xx} - S_{yy})/\dot{\epsilon}$ in uniaxial extension to remove the expected linear dependence on deformation rate at early times and low rates. The range of shear rates, $\dot{\gamma}$, and extension rates, $\dot{\epsilon}$, decrease by a factor of 5 from a maximum of 25 for the lowest curves in Figure 9. Units are given in terms of the relaxation time.

In start-up of shear flow, the orientation of the two most significant sections in the Cayley tree follow the established Doi−Edwards form at short times but deviate significantly at long times and high rates. After averaging over the segments (Figure 10a), the middle segment, 2, remains in linear response until the rate exceeds $\tau(1)^{-1}$. At these higher rates we can see "echoes" of the peak in segment 1 advected onto segment 2 as well as the expected nonlinearity in segment 2. Since it has a longer relaxation time, the averaged segment 1 orientation follows the nonlinear Doi−Edwards form over a wide range of rates, until effects of tube advection become significant. The advection widens the peak, delaying the return to isotropy for the whole segment until after the longest relaxation time. Looking at the orientation resolved in the y-variable reveals that advection can also have the opposite effect in shear. After segment 1 has relaxed from maximum orientation, segment 2 would start to respond nonlinearly. However, advected tube from segment 1 reduces the nonlinear orientation of segment 2 (Figure 11a).

As expected from H-polymer results,[2] above a rate of $\tau_{s,i}^{-1}$ in shear, segments stretch transiently and then decay to a steady-state value. At high rates the stretch can reach its maximum value for the current priority. Even so, at long times the stretch ratio will return to its steady value (if this is less than the priority). At the highest rates, segment 2 chains stretch, which allows the inner segments to stretch further (Figure 10b). Combining the orientation and stretch for each segment gives the transient shear viscosity shown in Figure 12. The broad transient peaks in shear arise from the advection, in association with the broad spectrum of relaxation times.

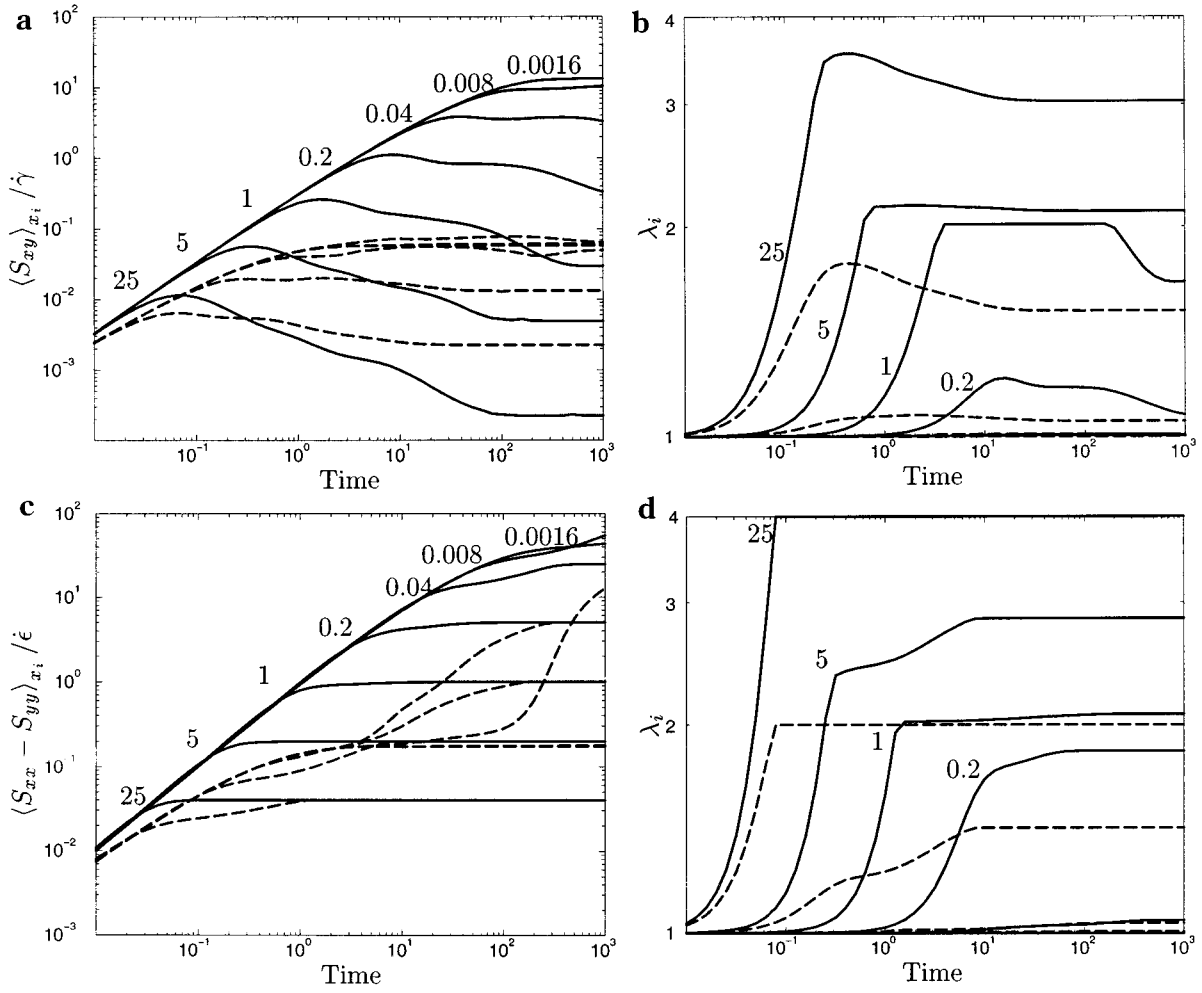

Figure 10. Stretch and orientation averaged over whole segment in startup flow for $q = (3, 2, 2)$, $s = (12, 6, 3)$ polymer. Curves are labeled by the deformation rate. (a) Orientation in simple shear. (b) Stretch in simple shear. (c) Orientation in uniaxial extension. (d) Stretch in uniaxial extension. The solid curve in each pair is from segment 1, and the dashed is from segment 2.

Extensional flows are an important test of polymer dynamics, mainly due to their ability to produce high molecular distortions. In uniaxial extension the averaged orientation again follows the standard Doi−Edwards curve, except at long times and high rates. Under these conditions advection pushes aligned tube out from segment 1 onto segment 2. This leads to the observed rapid rise of segment 2 orientation in Figure 10c. The general trend for stretching, as expected, is for limited stretch at low rates and a rapid rise to maximum stretch at high rates. However, more unusual features are also apparent in Figure 10d. At rates where segment 1 reaches its maximum stretch of $\lambda_1 = 2$, the next segment begins to stretch. Therefore, the maximum stretch of segment 1 is not constant at these rates. Outer segment stretching increases the priority of segment 1, allowing further stretching. At intermediate rates, the transient stretch of both segments has an interesting shape. This occurs when stretching is significant but the maximum has not yet been reached. The origin of these features is the orientational effect of tube advection. Again, the combined features of stretch and orientation give novel shapes in the transient viscosity. This is shown in Figure 12. After the onset of maximum stretch, the stretch coupling leads to a second rise in the extensional viscosity. This may not be seen in experiments, however, since the "knee" corresponding to the first attainment of maximum stretch has been identified with the necking instability in extensional flow.[25]

Finally, we compare the results of this work with the successful multimode pom-pom model.[4,5] The model successfully describes the nonlinear rheology of multiply branched polymer melts in transient shear, uniaxial, and planar extension with the same parameter set. A series of pom-pom elements are used describe various components of the multiply branched polymer. Applying the same approach to the Cayley tree provides an extreme test for the multimode pom-pom model.

Treating the results from our theory for the Cayley tree in the same way as experimental data, a multimode pom-pom fit is obtained. The multimode pom-pom equations are[5]

$$\boldsymbol{\sigma} = 3\sum_{i=1}^{p} g_i \lambda_i^{\,2}(t)\, \mathbf{S}_i(t) \tag{46}$$

$$\frac{D}{Dt}\lambda_i = \lambda_i(t)\, \mathbf{K}{:}\mathbf{S}_i - \frac{1}{\tau_{s,i}}(\lambda_i(t) - 1)e^{\nu^*(\lambda_i(t)-1)} \tag{47}$$

$$\frac{D}{Dt}\mathbf{A}_i = \mathbf{K}\cdot\mathbf{A}_i + \mathbf{A}_i\cdot\mathbf{K}^{\mathrm{T}} - \frac{1}{\tau_{b,i}}(\mathbf{A}_i - \mathbf{I}) \tag{48}$$

with $\mathbf{S}_i = \mathbf{A}_i/\mathrm{Tr}\ \mathbf{A}_i$ and maximum stretch condition $\lambda_i \leq q_i$. The four parameters g_i, $\tau_{b,i}$, $\tau_{s,i}$, and q_i for each of

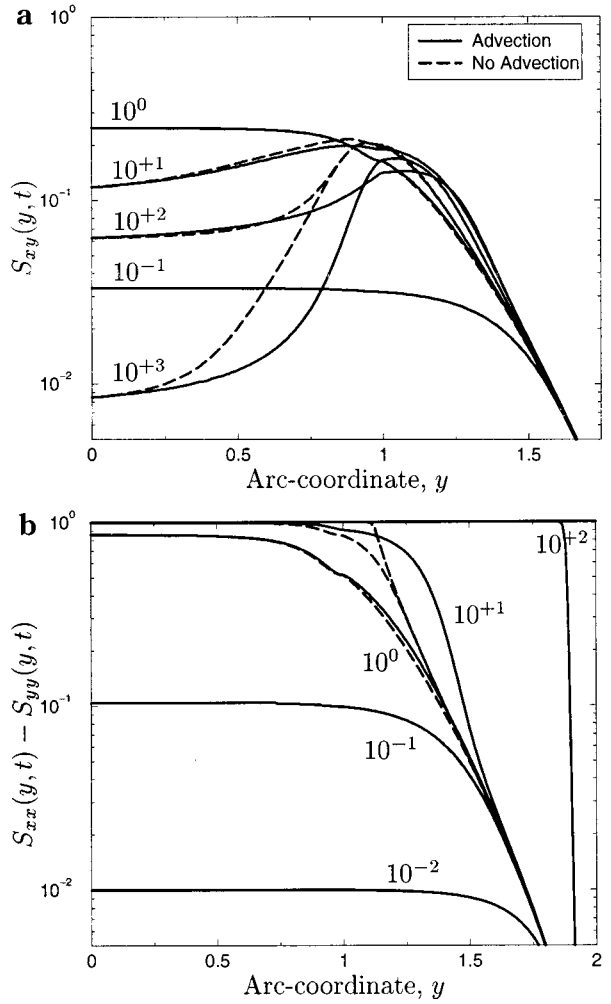

Figure 11. Orientation as a function of the arc coordinate y for $q = (3, 2, 2)$, $s = (12, 6, 3)$ polymer. (a) Shear. (b) Uniaxial extension. Curves are labeled by the time, and the deformation rate for all curves is $\tau(1)^{-1}$.

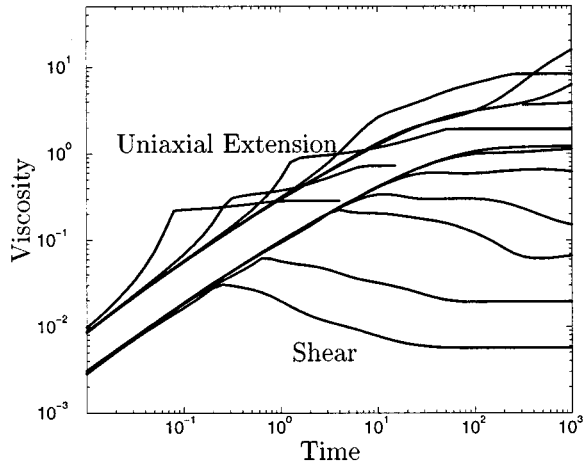

Figure 12. Transient viscosity for $q = (3, 2, 2)$, $s = (12, 6, 3)$ polymer. Note the characteristic shape from the stretching behavior. Rates decrease by a factor of 5, from 25 for the lowest curves, for both shear and uniaxial extension.

the p modes are chosen to fit the data. Linear rheology gives the mode amplitudes g_i and orientational relaxation times $\tau_{b,i}$, and the transient extensional data are typically used to give the stretch relaxation times $\tau_{s,i}$ and priorities q_i. We followed that strategy with $p = 4$, using three nonlinear modes and a single mode contributing a linear background. The results shown in Figure 13.

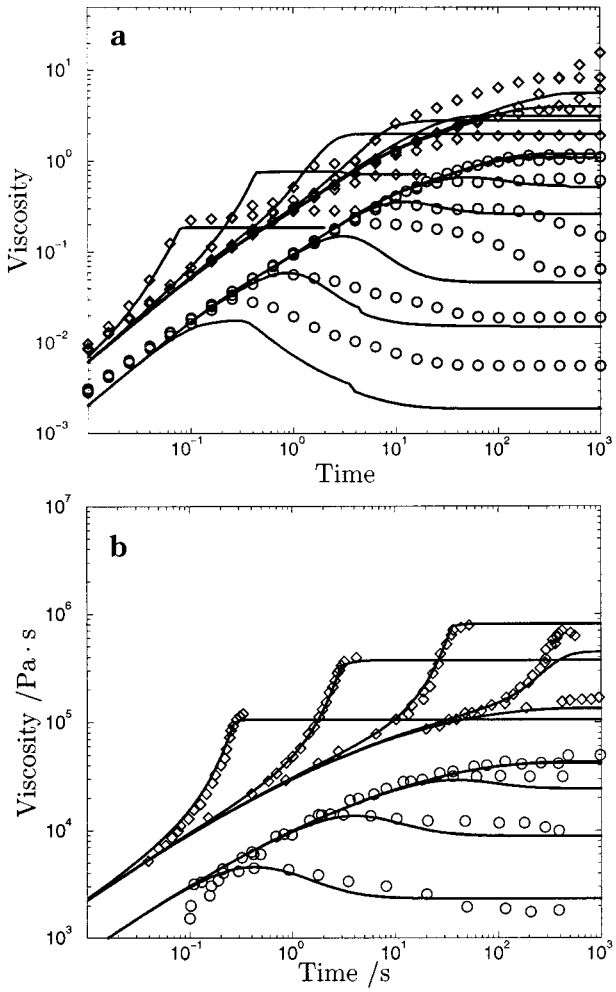

Figure 13. (a) Multimode pom-pom fitting of Cayley tree $q = (3, 2, 2)$, $s = (12, 6, 3)$. Points show the full Cayley tree calculations (the same data as Figure 12), and the solid lines are the pom-pom fit. The general trends are captured in the multimode fitting, yet features arising from the coupling between segments and the tube advection are missing. (b) A multimode fitting of the LDPE IUPAC-A is reproduced for comparison. Points are experimental data by Meissner[26] and Münstedt and Laun,[27] and the solid lines are a nine-mode pom-pom fit from Blackwell et al.[5]

Table 1. Parameters Used in the Four-Mode Pom-Pom Fit to the Cayley Tree Rheology

mode, i	g_i	$\tau_{b,i}$	$\tau_{s,i}$	q_i
1	7.625×10^{-1}	1.31×10^{-4}	1.31×10^{-5}	1
2	1.445×10^{-1}	2.00×10^{-1}	6.67×10^{-2}	2
3	7.700×10^{-2}	5.50×10^{0}	1.83×10^{0}	4
4	1.600×10^{-2}	$6.4 \times 10^{+1}$	8.00×10^{0}	4

The fitting procedure highlights a number of points about both the Cayley tree and the multimode pom-pom model. Relaxation times in the Cayley tree scale exponentially across each segment, yet a single time is used for each mode in the pom-pom fitting of the linear rheology. This means that it is impossible to identify a single pom-pom mode with each layer in the Cayley tree. Our three-mode fit required two pom-pom elements for the dominant inner layer, as shown in Table 1. This has implications for the choice of stretch parameters. Two stretch times are used to fit data produced with a single stretch time. Moreover, the stretch times could not be chosen to match the coupling of stretch between layers.

Therefore, either the first maximum stretch value, or the steady state, could be matched, but not both. Figure 13 shows the fit which matches the steady-state values at the higher rates shown. This highlights the lack of time-dependent priority in the multimode pom-pom model.

The multimode pom-pom model predicts the nonlinear shear curves. Departure points from the linear viscoelastic curve and the steady-state viscosities are reasonably well predicted by the four-mode pom-pom (Figure 13a). However, the shape of the transient shear curves in the four-mode fit are very different to the full Cayley tree calculation. The full calculations show a very broad peak and a trailing off in the stress growth coefficient at long times. These are not reproduced by the multimode pom-pom fit, which tends rapidly to a steady-state value. Tube advection is the main cause of the characteristic shapes in shear overshoots in the full model. The same features are also intriguingly present in experimental data on multiply branched polymers; one example is reproduced in Figure 13b. The LDPE data are taken by Meissner[26] and Münstedt and Laun,[27] and a nine-mode pom-pom fit, using the parameters from ref 5, is shown. The discrepancy between the pom-pom fit and the shear data in Figure 13b is of the same form as that between the pom-pom fit and the full Cayley tree calculations in Figure 13a. This strongly suggests that tube advection is also significant in commercial multiply branched polymers.

6. Discussion

The highly symmetric model branching structure permits calculation of the linear and nonlinear viscoelasticity for Cayley tree polymers. The star polymer relaxation method, activated diffusion along the primitive path, generalizes to this structure. Ideas developed for the pom-pom topology, namely the separation of stretch and orientation variables, also generalize to the Cayley tree but give novel coupling effects.

Inkson et al.[4] and Blackwell et al.[5] show that commercial LDPE can be modeled by a linear superposition of independent pom-pom modes. LDPE has a randomly branched topology. Each level of branching may be considered as an independent mode in the superposition. Our work shows that this picture needs to be modified in two ways. First, there is coupling between the different levels through the maximum stretch condition (42). Second, the orientation distribution varies with position along the segments. However, the effect of advection in flattening this distribution may reduce this effect.

Advection of tube along the polymer chain gives a coupling between the orientation in the various segments. Tube is moved, by advection, from one segment to the next. This causes outer segments to be more aligned than they would be in isolation, increasing their contribution to the stress in transient shear and steady-state extension. A comparison between nonlinear shear behavior in the Cayley tree and LDPE indicates that tube advection could be important for modeling commercial branched polymers. An advection coupling between the orientation of different pom-pom modes could be included in Inkson et al.'s model.[4]

These calculations highlight the extreme nature of treelike polymers. The exponential scaling of relaxation times on path length is significant. Chain segments of more than a few entanglement lengths give rise to experimentally inaccessible relaxation times. Also, if the volume fraction of outer segments is too high, the relaxation of inner segments will follow unentangled Rouse dynamics. These restrictions mean that, experimentally, entangled tree relaxation will be difficult to observe. Our study of entangled dynamics was necessarily restricted to a carefully chosen parameter set. This indicates that general branched polymers, such as LDPE, are likely to dynamically disentangle at some stage in their relaxation. Even when dynamic disentanglement does not occur, we have shown that the concentration of molecular weight in the outer layers can give a smaller viscosity than linear polymers with the same molecular weight.

Being such an extreme example, the theory for Cayley tree polymers suggests mechanisms that have more general relevance. Although commercial polymers like LDPE are not Cayley trees, many features of this theory are still relevant. Orientation should still be resolved along the chains, with tube advection being an important relaxation mechanism. Also, the coupling between the stretch of chains in various segments must be an important physical mechanism. Including these effects in a theory for asymmetric and irregular branched structures will be an important future step.

Characteristic features in the nonlinear rheology arise from these coupling effects. In systems such as LDPE, with polydispersity in topology and chain length, these features are not apparent. However, well-characterized polymers with the Cayley tree topology are expected to show these features. Experiments on the viscoelasticity of these polymers are awaited with interest.

Acknowledgment. R.J.B. acknowledges the financial support of the Frank Parkinson Fund at the University of Leeds and Corning Cables. The authors thank Daniel Read for his insightful comments.

Appendix A. Dynamic Dilution

Colby and Rubinstein[17] proposed that for Θ-solvents the entanglement molecular weight scales with polymer concentration, Φ, as $M_e(\Phi) = M_{e,0}/\Phi^{\alpha}$, with scaling exponent $\alpha = 4/3$. This result was applied to the dynamic dilution of polymer melts by Milner and McLeish,[1] who identified Φ as the fraction of unrelaxed chains. In our notation this becomes $\Phi_i(x_i) = u_{i-1} + \phi_i x_i$ when the relaxation has reached x_i. Using eq 3, the primitive chain step length increases as $a(\Phi) = a_0\Phi^{-\alpha/2}$ as the dilution progresses. Similarly, since the end-to-end length is fixed (2), the contour length measured with this step length decreases as $\bar{z}_i(\Phi) = (\nu/3)s_i a_0\Phi^{\alpha/2}$. The current contour length $z_i(t)$ scales in the same way so that the stretch ratio $z_i(t)/\bar{z}_i$ is unaffected by any change in the entanglement network.

Ball and McLeish[11] realized that these ideas lead to a renormalization of the spring potential (5) for star polymers. Their dynamic dilution result may be generalized to our Cayley tree polymer. Stress relaxation in star polymers is based on the idea of free ends retracting along the primitive path (see Figure 3). The elastic force introduced in section 1.1 acts as a barrier to this retraction. The energy required to compress the spring of force f_e (eq 6) is given by integrating f_e over the distance moved. However, as we noted above, the primitive path becomes shorter as the relaxation progresses while the ratio $z_i(t)/\bar{z}_i$ remains invariant. This effect must be included into the free energy cost of

retraction. It gives a smaller free energy cost than would otherwise be expected.

Starting with a polymer chain, of equilibrium length in segment i, moving the chain end to a point $z_i < \bar{z}_i$ has a free energy cost calculated as follows. Two effects of the dynamic dilution must be accounted for: the shorter path and a reduction in the spring force (6) through the step size a. Carefully choosing the integration variable as the invariant ratio gives

$$U_i(z_i/\bar{z}_i) = \int_1^{z_i/\bar{z}_i} \mathrm{d}(z_i'/\bar{z}_i) f_e(z_i'/\bar{z}_i,\Phi)\, \bar{z}_i(\Phi)$$

$$= \int_1^{z_i/\bar{z}_i} \mathrm{d}(z_i'/\bar{z}_i) \frac{3kT}{a_0\Phi^{-\alpha/2}}(z_i'/\bar{z}_i - 1)\frac{\nu}{3}s_i\Phi^{\alpha/2}a_0 \quad (49)$$

(this is the Ball−McLeish result[11]). Writing $\nu' s_i = U/kT$ and using our expression for the entanglement fraction $\Phi(z_i/\bar{z}_i)$ gives

$$\nu_i'(z_i/\bar{z}_i) = \frac{\nu}{\beta(\beta+1)\phi_i^2}\left(u_i^{\beta+1} - \left(u_{i-1} + \frac{z_i}{\bar{z}_i}\phi_i\right)^{\beta}\left(u_i + \beta\phi_i\left(1 - \frac{z_i}{\bar{z}_i}\right)\right)\right) \quad (50)$$

with $\beta = \alpha + 1$.

Noting that dynamic dilution does not apply to chain stretching ($z_i > \bar{z}_i$), since it gives no relaxation, we have a renormalized spring potential for chains in segment i:

$$\frac{U_i\left(\frac{z_i}{\bar{z}_i}\right)}{kT} = \begin{Bmatrix} \nu_i'(z_i/\bar{z}_i)s_i & \frac{z_i}{\bar{z}_i} < 1 \\ \frac{\nu}{2}s_i u_i^{\alpha}\left(\frac{z_i}{\bar{z}_i} - 1\right)^2 & \frac{z_i}{\bar{z}_i} > 1 \end{Bmatrix} \quad (51)$$

The condition for validity of dynamic dilution has been given recently, and we will return to test the validity of the assumption in Appendix B.

Appendix B. Validity of Dynamic Dilution

The calculations for the relaxation time in section 3 are based on the assumption that chains remain entangled. This permits the use of the dynamic dilution theory presented in Appendix A. Recently a condition has been given for the validity of dynamic dilution.[19] The dynamic dilution hypothesis is only valid where there is a smooth, exponential distribution of relaxation times. If the dilution occurs rapidly compared to the relaxation of the chain, then the relaxation dynamics are no longer in the entanglement regime. In that situation renormalized "Rouse tube" dynamics would be valid and provide the fastest relaxation mechanism.

The Cayley tree has a smooth distribution of relaxation times; however, we must still check that the dynamics remain entangled. For example, if there is a large mass fraction in the outer segments of the molecule, then the relaxation of innermost segments will have a very low entangled volume fraction. Relaxation of those segments would be dominated by renormalized Rouse dynamics.

We follow Milner et al.[19] in comparing two expressions for the rate of constraint release. Essentially we are looking for solution y to $t = \tau(y)$ to discover the arc coordinate where Rouse motion is no longer restricted by the tube. Rouse motion has mean monomer displacement $r \sim t^{1/4}$, so since tube dilation gives $a = a_0\Phi^{-\alpha/2}$ we have, setting $r(t) = a(t)$, $\Phi \sim t^{-1/2\alpha}$ and therefore

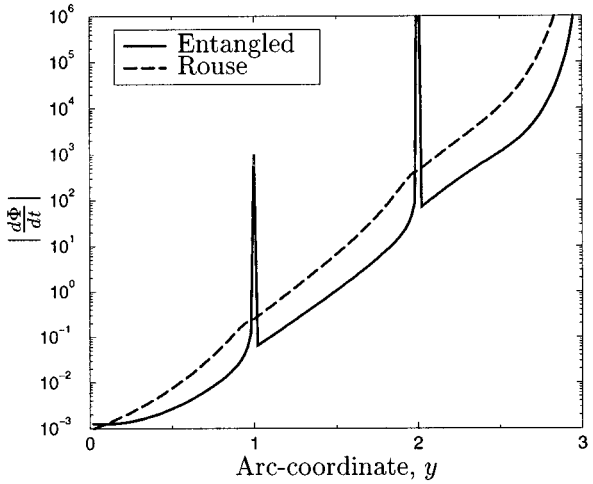

Figure 14. Entangled and Rouse rates of constraint release for $q = (3, 2, 2)$, $s = (12, 6, 3)$ polymer.

$$\left(\frac{\mathrm{d}\Phi}{\mathrm{d}t}\right)_{\text{Rouse}}(y) = -\frac{\Phi(y)}{2\alpha\tau(y)} \quad (52)$$

But our entangled dynamics has constraint release rate

$$\left(\frac{\mathrm{d}\Phi}{\mathrm{d}t}\right)_{\text{entangled}}(y) = \frac{\mathrm{d}\Phi}{\mathrm{d}y}\frac{\mathrm{d}y}{\mathrm{d}t} = \frac{\mathrm{d}\Phi}{\mathrm{d}y}\Big/\frac{\mathrm{d}\tau(y)}{\mathrm{d}y} \quad (53)$$

which can be calculated using eqs 17 and 26. So our assumption of dynamic dilution fails if the constraint release is faster than Rouse tube motion.

Figure 14 shows that the entangled dynamics are valid across our range of relaxation times, for the $q = (3, 2, 2)$, $s = (12, 6, 3)$ polymer. The divergence near the two intermediate branch points may be neglected. It is an artifact of our treatment of the relaxation at the large x end of each segment. In this region we have already assumed free diffusion by using the "early time" result (20) for the relaxation time. Very close to the center of the molecule (around $y = 0$) Figure 14 does show that a "disentanglement transition" should occur. Beyond the crossover point the assumed entangled dynamics are not valid. However, since the crossover is so close to the center of the molecule, this may reasonably be neglected. Thus, the relaxation times derived in section 3 are valid from this point of view.

Appendix C. Branch Point Withdrawal

Branch point withdrawal gives a third dynamic variable in the pom-pom model.[9] However, effects of branch point withdrawal on the rheology have been included in our dynamical equation for the orientation of the polymer chain (32). Although the branch point withdrawal distance, as a variable, is not required to calculate the stress, it can be measured in neutron scattering experiments.[2] A consideration of the reduction in drag resulting from branch point withdrawal also provides a useful insight into the maximum stretch condition.

Following Ajdari et al.,[20] we note that, where the local deformation rate exceeds the realignment rate, then polymer chains will become aligned. The immediate effect on the rheology has already been accounted for by including advection of the tube along the primitive

chain. However, this competition between deformation and relaxation also leads directly to the maximum stretch.

Physically, if polymer chain is pulled at a velocity faster than its motion by random steps, the chain will be drawn into the tube. The length of unaligned chain connected to the branch point which gives the drag force is reduced. A dynamical variable is introduced which measures the dimensionless distance to the unaligned friction blob, $w_i(t) \in [0,1]$ (Figure 7). Physically, this "blob" only contains monomers that have time to relax and explore new configurations, rather than being aligned by the flow. Since the relaxation time is a monotonically decreasing function of y, we expect that $w_i(t) > 0$ only if $w_j(t) = 1$ for all inner segments. This gives a single, well-defined boundary between aligned and unaligned segments.

On passing a branch point, this boundary gives the maximum stretch of the chains. We define the boundary by

$$v(w_i) = \frac{1}{2}\frac{\lambda_i a}{\tau_i(w_i)} \tag{54}$$

since chains align when pulled at speeds faster than the speed of random steps. Random steps of size $\lambda_i a$ occur in time τ_i but are equally likely to lie in either direction, so a factor of $^1/_2$ is included. This gives a reduction in the friction constant

$$\zeta_i(w_i) = 6kT\frac{q\tau_i(w_i)}{a^2} \tag{55}$$

Combining the two results gives a constant drag force $v(w_i)\zeta_i(w_i) = 3kT\lambda_i q_i/a$ to balance the elastic force in the stretch equation. Therefore, either the stretch of segments $i-1$ or the branch point withdrawal variable w_i evolves depending on the location of the boundary.

With our definition of w_i, the length of branch point withdrawn primitive path in segment i is $w_i z_i$. We also find that the stretch of the segment $i-1$ is coupled to the stretch of segment i via the force balance (see section 4.2). Using $v(z') = v_a(z') - z'$, with z' representing the distance to the branch point withdrawal point, gives

$$v(w_i) = \sum_{j<i} z_j \mathbf{K}:\ \int_0^1 \mathrm{d}x_j\, \mathbf{S}_j(x_j,t) + z_i\mathbf{K}:\ \int_0^{w_i}\mathrm{d}x_i\, \mathbf{S}_i(x_i,t) - \sum_{j<i}\dot{z}_j - z_i w_i \tag{56}$$

Combining this with eq 54, and substituting the inner segment stretch derivatives, gives the branch point withdrawal equation:

$$\frac{D}{Dt}w_i(t) = \frac{s_{i-1}}{\lambda_i(t)s_i\tau_{s,i-1}}(\lambda_{i-1}(t) - 1) + \mathbf{K}:\ \int_0^{w_i(t)}\mathrm{d}x_j\, \mathbf{S}_i(x_i,t) - \frac{\dot{\lambda}_i(t)}{\lambda_i(t)}w_i(t) - \frac{1}{2\frac{\nu}{3}s_i\tau_i(w_i(t))} \tag{57}$$

The initial condition for this differential equation is given by the limit of local branch point motion. Using the maximum stretch condition for segment $i-1$, this is

$$w_i(t_0) = \frac{6}{5s_i}\left(\lambda_i(t_0) - \frac{1}{q_i}\right) \tag{58}$$

Should this condition hold at a later time, the stretch of segment $i-1$ is no longer coupled to that of segment i. The stretch of segment $i-1$ should then be computed by eq 41.

In a full calculation both w_i and λ_i would be computed. However, for this paper we simply look at results for the rheology of Cayley tree polymers and leave the branch point withdrawal equation as stated. Solutions will be of the form presented in the original pom-pom paper by McLeish and Larson.[9]

References and Notes

(1) Milner, S. T.; McLeish, T. C. B. Parameter-free theory for stress relaxation in star polymer melts. *Macromolecules* **1997**, *30*, 2159−2166.

(2) McLeish, T. C. B.; Allgaier, J.; Bick, D. K.; Bishko, G.; Biswas, P.; Blackwell, R.; Blottière, B.; Clarke, N.; Gibbs, B.; Groves, D. J.; Hakiki, A.; Heenan, R. K.; Johnson, J. M.; Kant, R.; Read, D. J.; Young, R. N. Dynamics of entangled H-polymers: Theory, rheology and neutron scattering. *Macromolecules* **1999**, *32*, 6734−6758.

(3) Doi, M.; Edwards, S F. *The Theory of Polymer Dynamics*; Oxford University Press: Oxford, 1986.

(4) Inkson, N. J.; McLeish, T. C. B.; Harlen, O. G.; Groves, D. J. Predicting low-density polyethylene melt rheology in elongational and shear flows with "pom-pom" constitutive equations. *J. Rheol.* **1999**, *43*, 873−896.

(5) Blackwell, R. J.; McLeish, T. C. B.; Harlen, O. G. Molecular drag-strain coupling in branched polymer melts. *J. Rheol.* **2000**, *44*, 121−136.

(6) McLeish, T. C. B. Hierarchal relaxation in tube models of branched polymers. *Europhys. Lett.* **1988**, *6*, 511−516.

(7) Osaki, K. On the damping function of shear relaxation modulus for entangled polymers. *Rheol. Acta* **1993**, *32*, 429−437.

(8) Bick, D. K.; McLeish, T. C. B. Topological contributions to nonlinear elasticity in branched polymers. *Phys. Rev. Lett.* **1996**, *76*, 2587−2590.

(9) McLeish, T. C. B.; Larson, R. G. Molecular constitutive equations for a class of branched polymers: The pom-pom polymer. *J. Rheol.* **1998**, *42*, 81−110.

(10) Pearson, D. S.; Helfand, E. Viscoelastic properties of star-shaped polymers. *Macromolecules* **1984**, *17*, 888−895.

(11) Ball, R. C.; McLeish, T. C. B. Dynamic dilution and the viscosity of star polymer melts. *Macromolecules* **1989**, *22*, 1911−1913.

(12) McLeish, T. C. B. Molecular rheology of H-polymers. *Macromolecules* **1988**, *21*, 1062−1070.

(13) Rubinstein, M. Dynamics of ring polymers in the presence of fixed obstacles. *Phys. Rev. Lett.* **1986**, *57*, 3023−3027.

(14) Marrucci, G. In Mujumdar, A. S., Mashelkar, R. A., Eds.; *Advances in Transport Processes*; John Wiley: New York, 1984; Vol. 5.

(15) Klein, J. Dynamics of entangled linear, branched and cyclic polymers. *Macromolecules* **1986**, *19*, 105−118.

(16) Frischknecht, A. L.; Milner, S. T. Self-diffusion with dynamic dilution in star polymer melts. *Macromolecules* **2000**, *33*, 9764−9768.

(17) Colby, R. H.; Rubinstein, M. Two-parameter scaling for polymers in theta-solvents. *Macromolecules* **1990**, *23*, 2753−2757.

(18) Milner, S. T.; McLeish, T. C. B. Reptation and contour-length fluctuations in melts of linear polymers. *Phys. Rev. Lett.* **1998**, *81*, 725−728.

(19) Milner, S. T.; McLeich, T. C. B.; Young, R. N.; Hakiki, A.; Johnson, J. M. Dynamic dilution, constraint release, and star-linear blends. *Macromolecules* **1998**, *31*, 9345−9353.

(20) Ajdari, A.; Brochard-Wyart, F.; de Gennes, P.-G.; Leibler, L.; Viovy, J.-L.; Rubinstein, M. Slippage of an entangled polymer melt on a grafted surface. *Physica A* **1994**, *204*, 17−39.

(21) Marrucci, G. The Doi−Edwards model without independent alignment. *J. Non-Newtonian Fluid Mech.* **1986**, *21*, 329−336.

(22) Marrucci, G.; Grizzuti, N. The Doi−Edwards model in slow flows−predictions on the Weissenberg effect. *J. Non-Newtonian Fluid Mech.* **1986**, *21*, 319−328.

(23) Ferziger, J. H. *Numerical Methods for Engineering Application*; Wiley: New York, 1998.
(24) Yurasova, T. A.; McLeish, T. C. B.; Semenov, A. N. Stress relaxation in entangled comb polymer melts. *Macromolecules* **1994**, *27*, 7205−7211.
(25) McKinley, G. H.; Hassager, O. The Considère condition and rapid stretching of linear and branched polymer melts. *J. Rheol.* **1999**, *43*, 1195−1212.
(26) Meissner, J. Modification of the Weissenberg rheogoniometer for measurement of transient rheological properties of molten polyethylene under shear comparison with tensile data. *J. Appl. Polym. Sci.* **1972**, *16*, 2877−2899.
(27) Münstedt, H.; Laun, H. M. Elongation behaviour of a low-density polyethylene melt II. *Rheol. Acta* **1979**, *18*, 492−504.

MA001687A